Article

Progress in Physical Geography
2017, Vol. 41(6) 723–752

DOI: 10.1177/0309133317733667
journals.sagepub.com/home/ppg
SAGE

An illustrated introduction to general geomorphometry

Igor V Florinsky
Institute of Mathematical Problems of Biology, Keldysh Institute of Applied Mathematics, Russian Academy of Sciences, Russia

Abstract
Geomorphometry is widely used to solve various multiscale geoscientific problems. For the successful application of geomorphometric methods, a researcher should know the basic mathematical concepts of geomorphometry and be aware of the system of morphometric variables, as well as understand their physical, mathematical and geographical meanings. This paper reviews the basic mathematical concepts of general geomorphometry. First, we discuss the notion of the topographic surface and its limitations. Second, we present definitions, formulae and meanings for four main groups of morphometric variables, such as local, non-local, two-field specific and combined topographic attributes, and we review the following 29 fundamental morphometric variables: slope, aspect, northwardness, eastwardness, plan curvature, horizontal curvature, vertical curvature, difference curvature, horizontal excess curvature, vertical excess curvature, accumulation curvature, ring curvature, minimal curvature, maximal curvature, mean curvature, Gaussian curvature, unsphericity curvature, rotor, Laplacian, shape index, curvedness, horizontal curvature deflection, vertical curvature deflection, catchment area, dispersive area, reflectance, insolation, topographic index and stream power index. For illustrations, we use a digital elevation model (DEM) of Mount Ararat, extracted from the Shuttle Radar Topography Mission (SRTM) 1-arc-second DEM. The DEM was treated by a spectral analytical method. Finally, we briefly discuss the main paradox of general geomorphometry associated with the smoothness of the topographic surface and the non-smoothness of the real topography; application of morphometric variables; statistical aspects of geomorphometric modelling, including relationships between morphometric variables and roughness indices; and some pending problems of general geomorphometry (i.e. analysis of inner surfaces of caves, analytical description of non-local attributes and structural lines, as well as modelling on a triaxial ellipsoid). The paper can be used as a reference guide on general geomorphometry.

Keywords
Topography, geomorphometry, morphometric variable, surface, curvature, digital terrain modelling, spectral analytical method

1 Introduction

Topography is one of the main factors controlling processes taking place in the near-surface layer of the planet. In particular, it is one of the soil forming factors (Gerrard, 1981) influencing: (1) climatic and meteorological characteristics, which control hydrological and thermal

Corresponding author:
Igor V Florinsky, Institute of Mathematical Problems of Biology, The Keldysh Institute of Applied Mathematics, Russian Academy of Sciences, Pushchino, Moscow Region, 142290, Russia.
Email: iflor@mail.ru

regimes of soils (Geiger, 1966); (2) prerequisites for gravity-driven overland and intrasoil lateral transport of water and other substances (Kirkby and Chorley, 1967); (3) spatial distribution of vegetation cover (Franklin, 1995); and (4) ecological patterns and processes (Ettema and Wardle, 2002). At the same time, being a result of the interaction of endogenous and exogenous processes of different scales, topography reflects the geological structure of a terrain (Brocklehurst, 2010; Burbank and Anderson, 2012).

Given this connection, qualitative and quantitative topographic information is widely used in the geosciences. Before the 1990s, topographic maps were the main source of quantitative information on topography. They were analysed using conventional geomorphometric techniques to calculate morphometric variables (e.g. slope and drainage density) and produce morphometric maps (Clarke, 1966; Gardiner and Park, 1978; Horton, 1945; Lastochkin, 1987; Mark, 1975; Strahler, 1957; Volkov, 1950). In the mid-1950s, a new research field – digital terrain modelling – emerged in photogrammetry (Miller and Leflamme, 1958; Rosenberg, 1955). DEMs (digital elevation models), two-dimensional discrete functions of elevation, became the main source of information on topography. Subsequent advances in computer, space and geophysical technologies were responsible for the transition from conventional to digital geomorphometry (Burrough, 1986; Dikau, 1988; Evans, 1972). This was substantially supported by the development of the physical and mathematical theory of the topographic surface (Evans, 1972, 1980; Gallant and Hutchinson, 2011; Jenčo, 1992; Jenčo et al., 2009; Krcho, 1973, 2001; Shary, 1991, 1995; Shary et al., 2002, 2005). As a result, geomorphometry evolved into the science of quantitative modelling and analysis of the topographic surface and relationships between topography and other natural and artificial components of geosystems.

Currently, geomorphometric methods are widely used to solve various multiscale problems of geomorphology, hydrology, remote sensing, soil science, geology, geophysics, geobotany, glaciology, oceanology, climatology, planetology and other disciplines; see reviews (Clarke and Romero, 2017; Deng, 2007; Florinsky, 1998b; Jordan, 2007; Lecours et al., 2016; Minár et al., 2016; Moore et al., 1991; Pike, 2000; Wasklewicz et al., 2013; Wilson, 2012) and books (Florinsky, 2016; Hengl and Reuter, 2009; Li et al., 2005; Wilson and Gallant, 2000).

For the successful application of geomorphometric modelling, a researcher should know the basic mathematical concepts of general geomorphometry, be aware of the system of morphometric variables and understand their physical, mathematical and geographical meanings. The aim of this paper is to review these key issues of general geomorphometry.

II Topographic surface

Real surfaces of land or submarine topography are not smooth and regular. A rigorous mathematical treatment of such surfaces can be problematic. However, in practice, it is sufficient to approximate a real surface by the topographic surface. The topographic surface is a closed, oriented, continuously differentiable, two-dimensional manifold S in the three-dimensional Euclidean space E^3.

There are five limitations valid for the topographic surface (Evans, 1980; Shary, 1995):

1. The topographic surface is uniquely defined by a continuous, single-valued bivariate function

$$z = f(x, y) \qquad (1)$$

   where z is elevation and x and y are the Cartesian coordinates. This means that caves, grottos and similar landforms are excluded.

2. The elevation function in equation (1) is smooth. This means that the topographic surface has derivatives of all orders. In practice, the first (p and q), second (r, t and s) and third (g, h, k and m) partial derivatives of elevation are used

$$p = \frac{\partial z}{\partial x}, \quad q = \frac{\partial z}{\partial y},$$
$$r = \frac{\partial^2 z}{\partial x^2}, \quad t = \frac{\partial^2 z}{\partial y^2}, \quad s = \frac{\partial^2 z}{\partial x \partial y},$$
$$g = \frac{\partial^3 z}{\partial x^3}, \quad h = \frac{\partial^3 z}{\partial y^3}, \quad k = \frac{\partial^3 z}{\partial x^2 \partial y}, \quad m = \frac{\partial^3 z}{\partial x \partial y^2} \tag{2}$$

3. The topographic surface is located in a uniform gravitational field. This limitation is realistic for sufficiently small portions of the geoid, when the equipotential surface can be considered as a plane.
4. The planimetric sizes of the topographic surface are essentially less than the radius of the planet. It is usually assumed that the curvature of the planet may be ignored if the size of the surface portion is less than at least 0.1 of the average planetary radius. In computations, either sizes of moving windows in local computational methods or sizes of the entire area in global computational methods must comply with this condition (see section 3.2).
5. The topographic surface is a scale-dependent surface (Clarke, 1988). This means that a fractal component of topography is considered as a high-frequency noise.

III Morphometric variables

3.1 General

A morphometric (or topographic) variable (or attribute) is a single-valued bivariate function $\omega = u(x, y)$ describing properties of the topographic surface.

In this paper, we review fundamental topographic variables associated with the theory of the topographic surface and the concept of general geomorphometry, which is defined as 'the measurement and analysis of those characteristics of landform which are applicable to any continuous rough surface.... General geomorphometry as a whole provides a basis for the quantitative comparison ... of qualitatively different landscapes ....' (Evans, 1972: 18).

There are several classifications of morphometric variables based on their intrinsic (mathematical) properties (Evans and Minár, 2011; Florinsky, 1998b, 2016: ch 2; Minár et al., 2016; Shary, 1995; Shary et al., 2002). Here, we use a modified classification of Florinsky (2016: ch 2) adopting some ideas of Evans and Minár (2011).

Morphometric variables can be divided into four main classes (Table 1): (1) local variables; (2) non-local variables; (3) two-field specific variables; and (4) combined variables. The terms 'local' and 'non-local' are used regardless of the study scale or model resolution. They are associated with the mathematical sense of a variable (c.f. the definitions of a local and a non-local variable – see sections 3.2 and 3.3). Being a morphometric variable, elevation does not belong to any class listed, but all topographic attributes are derived from DEMs.

3.2 Local morphometric variables

A local morphometric variable is a single-valued bivariate function describing the geometry of the topographic surface in the vicinity of a given point of the surface (Speight, 1974) along directions determined by one of the two pairs of mutually perpendicular normal sections (Figure 1(a) and (b)).

A normal section is a curve formed by the intersection of a surface with a plane containing the normal to the surface at a given point (Pogorelov, 1957). At each point of the topographic surface, an infinite number of normal

Table 1. Classification of morphometric variables.

Local variables			Non-local variables	Two-field specific variables	Combined variables
	Flow attributes	*Form attributes*			
First-order variables	G		CA	R	TI
	A		DA	I	SI
	A_N				
	A_E				
Second-order variables	k_p	k_{min}			
	k_h	k_{max}			
	k_v	H			
	E	K			
	k_{he}	M			
	k_{ve}	∇^2			
	K_a	IS			
	K_r	C			
	rot				
Third-order variables	D_{kh}				
	D_{kv}				

sections can be constructed, but only two pairs of them are important for geomorphometry.

The first pair of mutually perpendicular normal sections includes two principal sections (Figure 1(a)) well known from differential geometry (Pogorelov, 1957). These are normal sections with extreme – maximal and minimal – bending at a given point of the surface.

The second pair of mutually perpendicular normal sections includes two ones (Figure 1(b)) dictated by gravity (Shary, 1991). One of these two sections includes the gravitational acceleration vector and has a common tangent line with a slope line[1] at a given point of the topographic surface. The other section is perpendicular to the first one and tangential to a contour line at a given point of the topographic surface.

Local variables are divided into two types (see Table 1) – form and flow attributes – which are related to the two pairs of normal sections (Shary, 1995; Shary et al., 2002).

Form attributes are associated with two principal sections. These attributes are gravity field invariants. This means that they do not depend on the direction of the gravitational acceleration vector. Among these are minimal curvature (k_{min}), maximal curvature (k_{max}), mean curvature (H), the Gaussian curvature (K), unsphericity curvature (M), Laplacian (∇^2), shape index (IS), curvedness (C) and some others.

Flow attributes are associated with two sections dictated by gravity. These attributes are gravity-field specific variables. Among these are slope (G), aspect (A), northwardness (A_N), eastwardness (A_E), plan curvature (k_p), horizontal curvature (k_h), vertical curvature (k_v), difference curvature (E), horizontal excess curvature (k_{he}), vertical excess curvature (k_{ve}), accumulation curvature (K_a), ring curvature (K_r), rotor (rot), horizontal curvature deflection (D_{kh}), vertical curvature deflection (D_{kv}) and some others.

K, K_a and K_r are total curvatures; k_{min}, k_{max}, k_h, k_v, k_{he} and k_{ve} are simple curvatures; and H, M and E are independent curvatures. Total and simple curvatures can be expressed by elementary formulae using the independent curvatures (Shary, 1995) (see equations (9)–(15) and

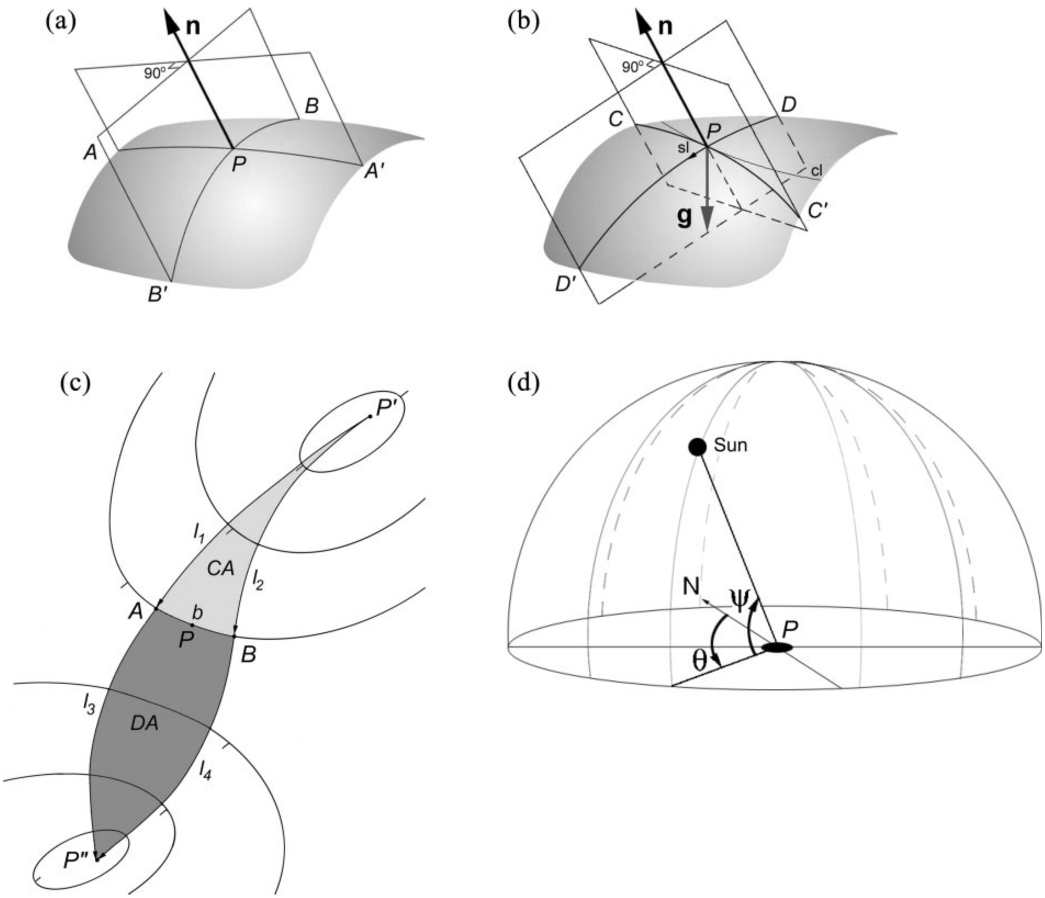

Figure 1. Schemes for the definitions of local, non-local and two-field specific variables. (a) and (b) display two pairs of mutually perpendicular normal sections at a point *P* of the topographic surface: (a) Principal sections *APA′* and *BPB′*; (b) Sections *CPC′* and *DPD′* allocated by gravity, **n** is the external normal, **g** is the gravitational acceleration vector, *cl* is the contour line, *sl* is the slope line. (c) Catchment and dispersive areas, *CA* and *DA*, are areas of figures *P′AB* (light grey) and *P″AB* (dark grey), correspondingly; *b* is the length of a contour line segment *AB*; l_1, l_2, l_3 and l_4 are the lengths of slope lines *P′A*, *P′B*, *AP″* and *BP″*, correspondingly. (d) The position of the Sun in the sky: θ is solar azimuth angle, ψ is solar elevation angle, and N is north direction.

(19)–(23)). These 12 attributes constitute a complete system of curvatures (Shary, 1995).

Local topographic variables are functions of the partial derivatives of elevation (see equations (4)–(26)). In this regard, local variables can be divided into three groups (Evans and Minár, 2011) (see Table 1): (1) first-order variables – G, A, A_N and A_E – are functions of only the first derivatives; (2) second-order variables – k_{min}, k_{max}, H, K, M, ∇^2, IS, C, k_p, k_h, k_v, E, k_{he}, k_{ve}, K_a, K_r and rot – are functions of both the first and second derivatives; and (3) third-order variables – D_{kh} and D_{kv} – are functions of the first, second and third derivatives.

The partial derivatives of elevation (and thus local morphometric variables) can be estimated from DEMs by: (1) several finite-difference methods using 3 × 3 or 5 × 5 moving windows (Evans, 1979, 1980; Florinsky, 1998c, 2009; Minár et al., 2013; Shary, 1995; Shary et al., 2002; Zevenbergen and Thorne, 1987); and (2) analytical computations based on DEM interpolation by local splines (Mitášová and Mitáš, 1993) or global approximation of a DEM by high-order orthogonal polynomials (Florinsky and Pankratov, 2016). Comparison of the methods can be found elsewhere (Florinsky, 1998a; Pacina, 2010; Schmidt et al., 2003).

3.3 Non-local morphometric variables

A non-local (or regional) morphometric variable is a single-valued bivariate function describing a relative position of a given point on the topographic surface (Speight, 1974).

Among non-local topographic variables are catchment area (CA) and dispersive area (DA). To determine non-local morphometric attributes, one should analyse a relatively large territory with boundaries located far away from a given point (e.g. an entire upslope portion of a watershed) (Figure 1(c)).

Flow routing algorithms are usually applied to estimate non-local variables. These algorithms determine a route along which a flow is distributed from a given point of the topographic surface to downslope points. There are several flow routing algorithms grouped into two types: (1) eight-node single-flow direction (D8) algorithms using one of the eight possible directions separated by 45° to model a flow from a given point (Jenson and Domingue, 1988; Martz and de Jong, 1988); and (2) multiple-flow direction (MFD) algorithms using the flow partitioning (Freeman, 1991; Quinn et al., 1991). There are some methods combining D8 and MFD principles (Tarboton, 1997). Comparison of the algorithms can be found elsewhere (Huang and Lee, 2016; Orlandini et al., 2012; Wilson et al., 2008).

3.4 Two-field specific morphometric variables

A two-field specific morphometric variable is a single-valued bivariate function describing relations between the topographic surface (located in the gravity field) and other fields, in particular solar irradiation and wind flow (Evans and Minár, 2011).

Among two-field specific morphometric variables are reflectance (R) and insolation (I). These variables are functions of the first partial derivatives of elevation (see equation (2)) and angles describing the position of the Sun in the sky (Figure 1(d)). Reflectance and insolation can be derived from DEMs using methods for the calculation of local variables (see section 3.2).

Openness (Yokoyama et al., 2002), incorporating the viewshed concept (Fisher, 1996), is also a two-field specific variable. In this case, the second field is a set of unobstructed sightlines between a given point of the topographic surface and surrounding points.

3.5 Combined morphometric variables

Morphometric variables can be composed from local and non-local variables. Such attributes consider both the local geometry of the topographic surface and a relative position of a point on the surface.

Among combined morphometric variables are topographic index (TI), stream power index (SI) and some others. Combined variables are derived from DEMs by the sequential application of methods for non-local and local variables, followed by a combination of the results.

IV Brief description and illustration of morphometric variables

4.1 Data and methods

To illustrate mathematical concepts of geomorphometry, we used a DEM of Mount Ararat (Figure 2). The area is located between 44.2° and 44.5° E, and 39.6° and 39.8° N (the area size is $18' \times 12'$, that is, 25.725 km × 22.204 km). A spheroidal equal angular DEM was extracted from the quasi-global Shuttle Radar Topography Mission (SRTM) 1-arc-second DEM (Farr et al., 2007; USGS, 2015). The DEM includes 779,401 points (the matrix

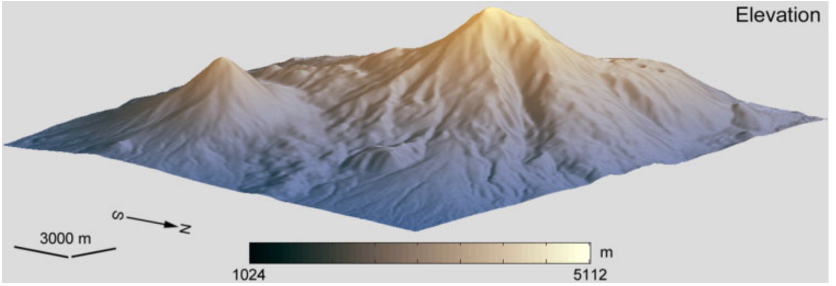

Figure 2. Mount Ararat, elevation.

1081×721). The grid spacing is $1''$, that is, the linear sizes of the $1'' \times 1''$ cell are 23.82 m $\times$ 30.84 m at the mean latitude, 39.7° N.

Elevation approximation and derivation of local and two-field specific variables were carried out by the recently developed spectral analytical method (Florinsky and Pankratov, 2016). The method is intended for the processing of regularly spaced DEMs within a single framework including DEM global approximation, denoising, generalization and calculation of the partial derivatives of elevation. The method is based on high-order orthogonal expansions using the Chebyshev polynomials with the subsequent Fejér summation. In this study, we used 300 expansion coefficients of the original elevation function by the Chebyshev polynomials by both x- and y-axes. Calculation of non-local variables was performed by the Martz–de Jong flow routing algorithm (Martz and de Jong, 1988) adapted to spheroidal equal angular grids (Florinsky, 2017a). To derive combined morphometric variables, we sequentially applied the Martz–de Jong algorithm adapted to spheroidal equal angular grids and the spectral analytical method.

Wide dynamic ranges characterize the second- and third-order local variables as well as non-local attributes. To avoid loss of information on the spatial distribution of their values in mapping, a logarithmic transform should be applied (Shary et al., 2002)

$$\Theta' = \mathrm{sign}(\Theta)\ln(1 + 10^{nm}|\Theta|) \qquad (3)$$

where Θ' and Θ are transformed and original values of a variable; $n = 0$ for the non-local variables; $n = 2, \ldots, 9$ for the second- and third-order local variables; $m = 2$ for the total curvatures and third-order local variables, $m = 1$ for other variables. Such a transformation considers that: (1) dynamic ranges of some attributes include both positive and negative values; and (2) correct mapping of variables from different classes and groups require different exponent values for the same territory and DEM resolution. In the spectral analytical method, selection of the n value depends on the size of a study area. In our case, $n = 4$ for third-order variables and $n = 5$ for second-order ones.

For the three-dimensional (3D) visualization of morphometric models, we used a $2^{\times}$ vertical exaggeration and a viewpoint with 45° azimuth and 35° elevation.

To evaluate statistical interrelationships between 12 attributes of the complete system of curvatures, we performed multiple Spearman's rank correlation analysis of their models (Table 2). Rank correlations allow the consideration of possible non-normality in curvature distributions. The sample size was 7000 points (the matrix 100×70); the grid spacing was $10''$.

Data processing was conducted with the software Matlab R2008b (©The MathWorks Inc. 1984–2008) and LandLord 4.0 (Florinsky, 2016: 413–414). Statistical analysis was carried out by Statgraphics Plus 3.0 (©Statistical Graphics Corp. 1994–1997).

Table 2. Spearman's rank correlations between 12 attributes of the complete system of curvatures for the Mount Ararat models.

	k_h	k_v	k_{he}	k_{ve}	E	K_a	K_r	k_{min}	k_{max}	K	H	M
k_h		0.36	0.58	–0.56	–0.72	–0.07	—	0.74	0.79	–0.05	0.88	0.04
k_v	0.36		–0.26	0.20	0.29	0.04	—	0.68	0.63	0.05	0.72	–0.06
k_{he}	0.58	–0.26		–0.31	–0.81	—	0.49	—	0.49	–0.27	0.28	0.56
k_{ve}	–0.56	0.20	–0.31		0.73	0.17	0.58	–0.47	–0.06	–0.14	–0.30	0.49
E	–0.72	0.29	–0.81	0.73		0.11	—	–0.26	–0.36	0.10	–0.36	–0.10
K_a	–0.07	0.04	—	0.17	0.11		0.19	0.12	–0.17	0.78	–0.02	—
K_r	—	—	0.49	0.58	—	0.19		–0.33	0.28	–0.27	—	0.71
k_{min}	0.74	0.68	—	–0.47	–0.26	0.12	–0.33		0.55	0.30	0.86	–0.43
k_{max}	0.79	0.63	0.49	–0.06	–0.36	–0.17	0.28	0.55		–0.32	0.87	0.40
K	–0.05	0.05	–0.27	–0.14	0.10	0.78	–0.27	0.30	–0.32		—	–0.38
H	0.88	0.72	0.28	–0.30	–0.36	–0.02	—	0.86	0.87	—		—
M	0.04	–0.06	0.56	0.49	–0.10	—	0.71	–0.43	0.40	–0.38	—	

*$P \leq 0.05$ for statistically significant correlations; dashes are statistically insignificant correlations.

4.2 Local morphometric variables: flow attributes

1. Slope (G) is an angle between the tangential and horizontal planes at a given point of the topographic surface (Shary, 1991)

$$G = \arctan\sqrt{p^2 + q^2} \tag{4}$$

Slope is a non-negative variable ranging from 0 to 90. The unit of G is degree. Slope (Figure 3(a)) determines the velocity of gravity-driven flows.

2. Aspect (A) is an angle between the northern direction and the horizontal projection of the two-dimensional vector of gradient counted clockwise at a given point of the topographic surface (Shary et al., 2002)

$$\begin{aligned} A = & -90[1 - \mathrm{sign}(q)](1 - |\mathrm{sign}(p)|) \\ & + 180[1 + \mathrm{sign}(p)] \\ & - \frac{180}{\pi}\mathrm{sign}(p)\arccos\left(\frac{-q}{\sqrt{p^2 + q^2}}\right) \end{aligned} \tag{5}$$

Aspect is a non-negative variable ranging from 0 to 360. The unit of A is degree. Aspect (Figure 3(b)) is a measure of the direction of gravity-driven flows.

3. Northwardness and eastwardness aspect is a circular variable: its values range from 0° to 360°, and both of these values correspond to the north direction. Therefore, A cannot be used in linear statistical analysis. To avoid this problem, two auxiliary local indices can be applied: northwardness (A_N) and eastwardness (A_E) (Mardia, 1972)

$$A_N = \cos A \tag{6}$$

$$A_E = \sin A \tag{7}$$

Northwardness (Figure 3(c)) and eastwardness (Figure 3(d)) are dimensionless variables. A_N is equal to 1, –1 and 0 on the northern, southern and eastern/western slopes, correspondingly. A_E is equal to 1, –1 and 0 on the eastern, western and northern/southern slopes, correspondingly. These variables accentuate northern/southern and eastern/western trends in the spatial distribution of slopes.

4. Plan curvature (k_p) is the curvature of a contour line at a given point of the

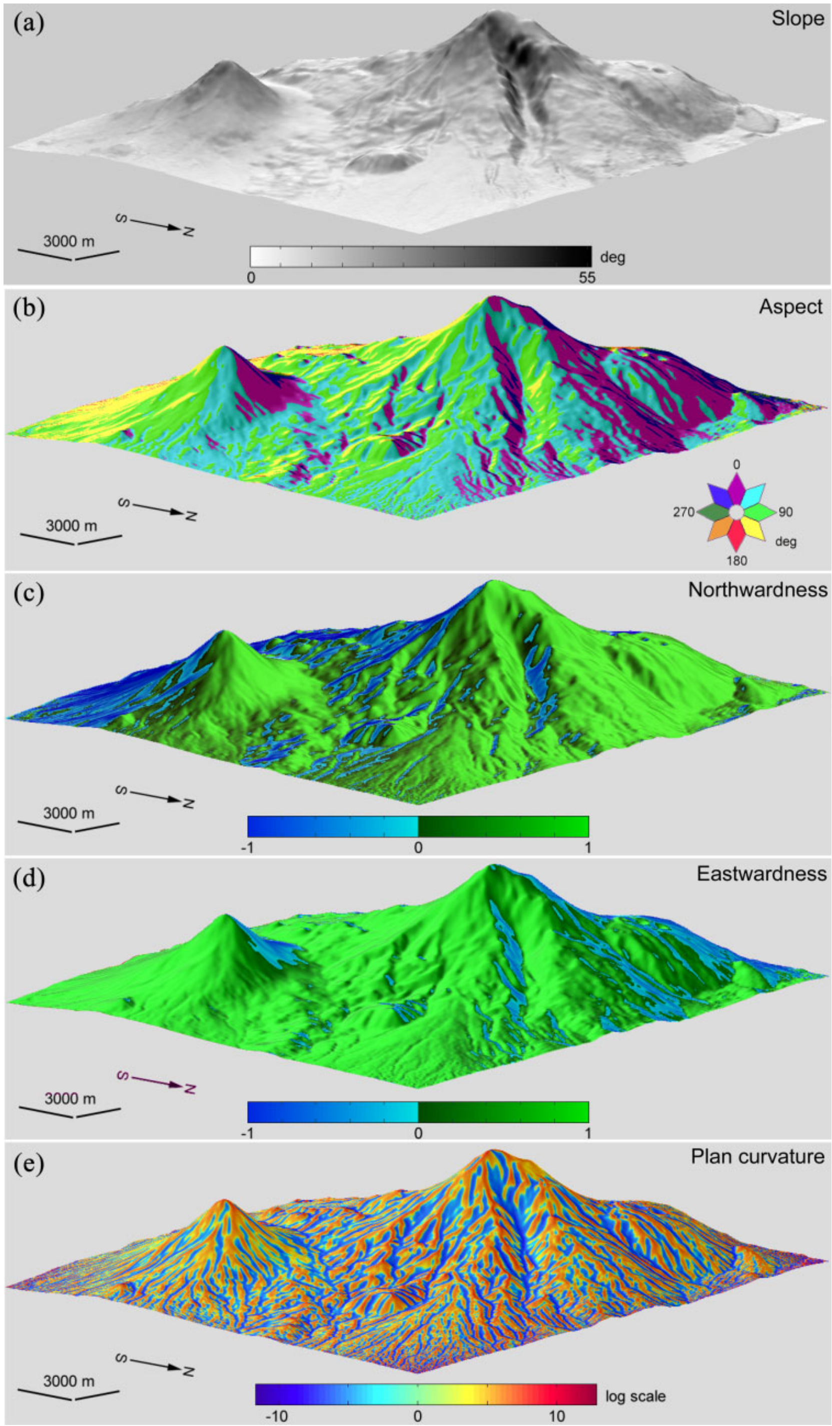

Figure 3. Mount Ararat, local variables, flow attributes: (a) slope; (b) aspect; (c) northwardness; (d) eastwardness; (e) plan curvature; (f) horizontal curvature; (g) vertical curvature; (h) difference curvature; (i) horizontal excess curvature; (j) vertical excess curvature; (k) accumulation curvature; (l) ring curvature; (m) rotor; (n) horizontal curvature deflection; (o) vertical curvature deflection.

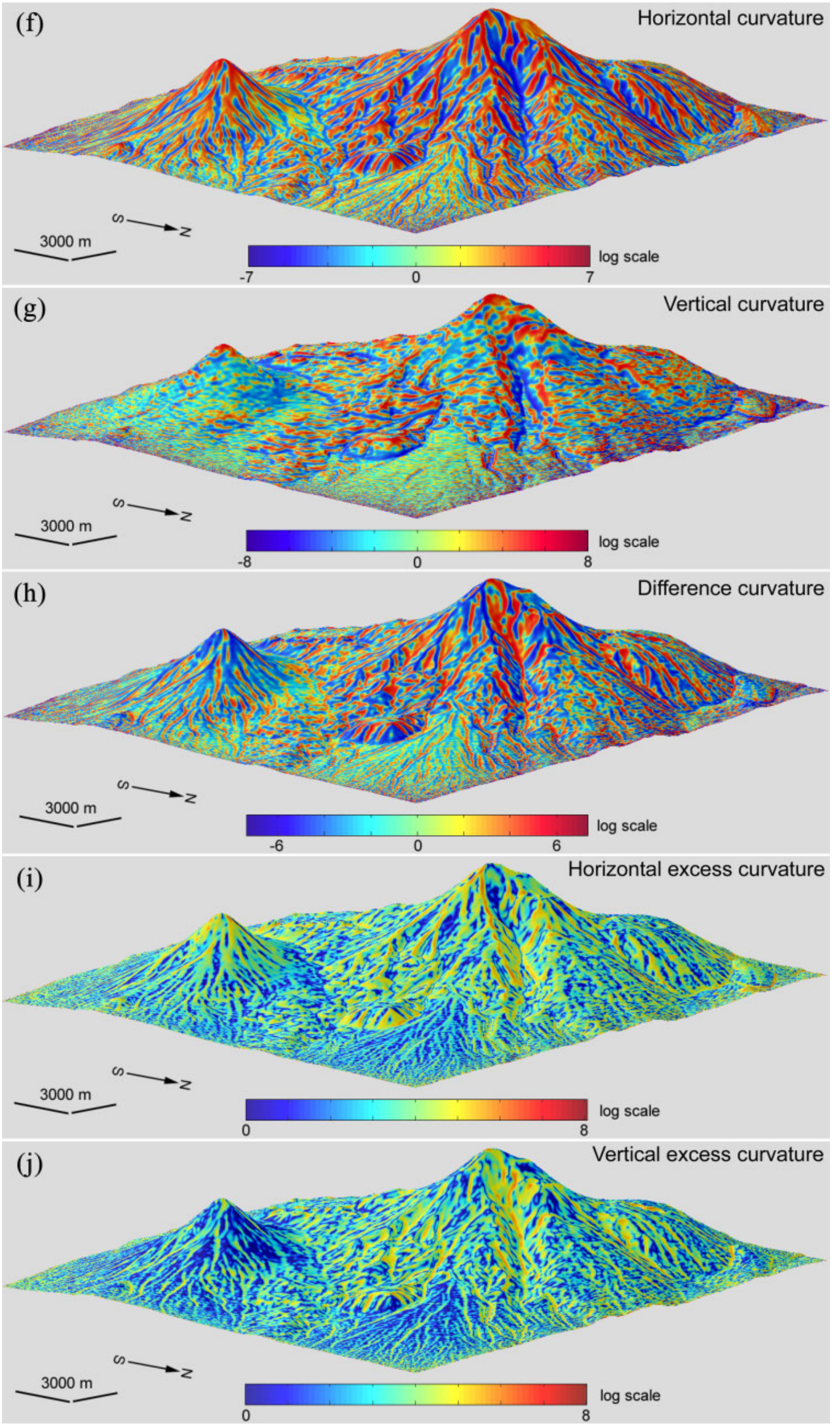

Figure 3. (Continued)

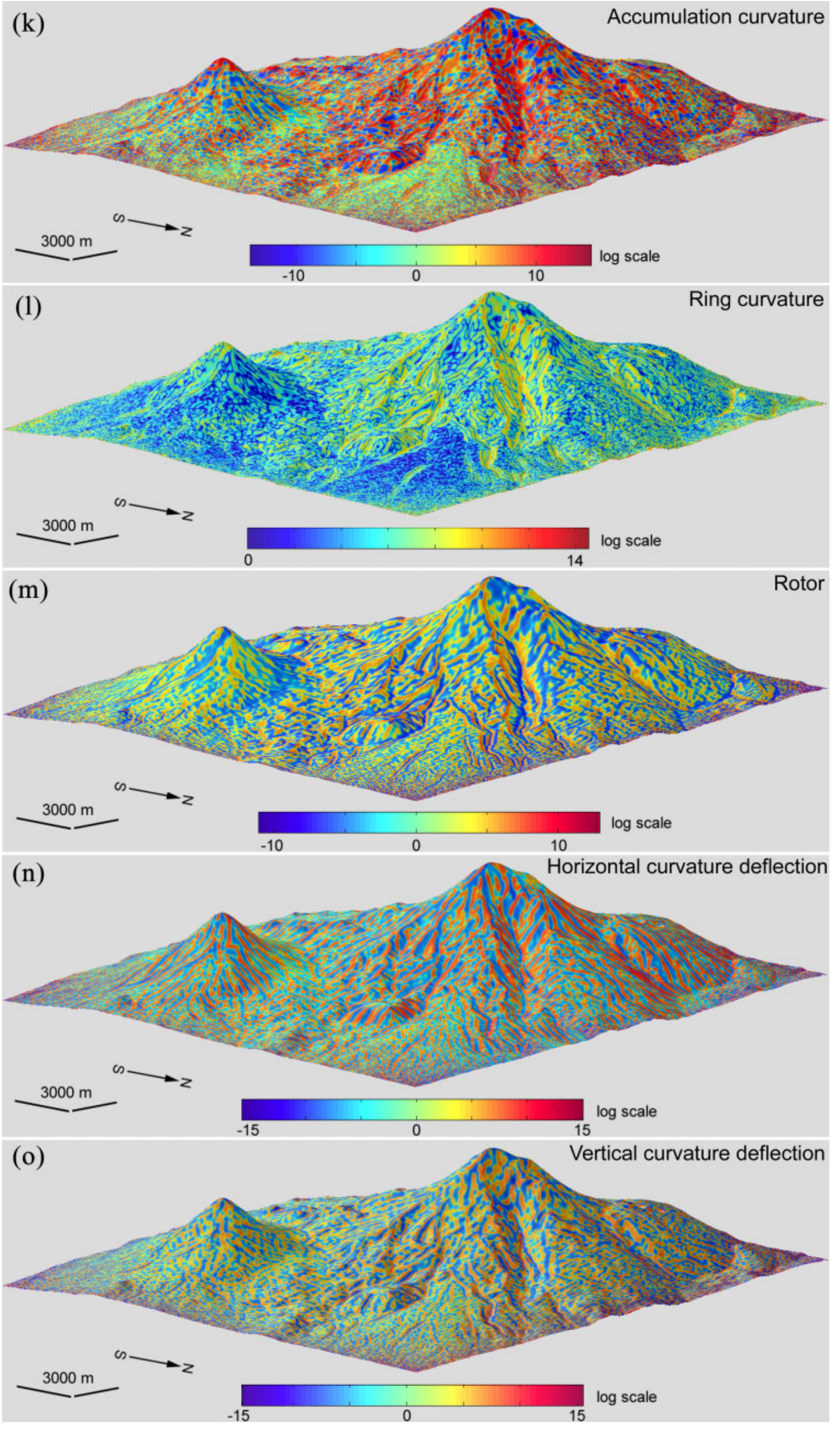

Figure 3. (Continued)

topographic surface (Evans, 1979; Krcho, 1973)

$$k_p = -\frac{q^2r - 2pqs + p^2t}{\sqrt{(p^2+q^2)^3}} \quad (8)$$

This variable can be positive, negative or zero. The unit of k_p is m^{-1}. Plan curvature (Figure 3(e)) is a measure of flow line[2] divergence. Flow lines converge where $k_p < 0$ and diverge where $k_p > 0$; $k_p = 0$ refers to parallel flow lines.

5. Horizontal (or tangential) curvature (k_h) is the curvature of a normal section tangential to a contour line (Figure 1(b)) at a given point of the topographic surface (Krcho, 1983; Shary, 1991)

$$k_h = -\frac{q^2r - 2pqs + p^2t}{(p^2+q^2)\sqrt{1+p^2+q^2}} \quad (9)$$

This variable can be positive, negative or zero. The unit of k_h is m^{-1}. Horizontal curvature (Figure 3(f)) is a measure of flow convergence (one of the two mechanisms of flow accumulation): gravity-driven overland and intrasoil lateral flows converge where $k_h < 0$, and they diverge where $k_h > 0$. Geomorphologically, k_h mapping allows revealing ridge and valley spurs (divergence and convergence areas, correspondingly).

6. Vertical (or profile) curvature (k_v) is the curvature of a normal section having a common tangent line with a slope line (Figure 1(b)) at a given point of the topographic surface (Aandahl, 1948; Shary, 1991; Speight, 1974)

$$k_v = -\frac{p^2r + 2pqs + q^2t}{(p^2+q^2)\sqrt{(1+p^2+q^2)^3}} \quad (10)$$

This variable can be positive, negative or zero. The unit of k_v is m^{-1}. Vertical curvature (Figure 3(g)) is a measure of relative deceleration and acceleration of gravity-driven flows (one of the two mechanisms of flow accumulation). Overland and intrasoil lateral flows are decelerated where $k_v < 0$, and they are accelerated where $k_v > 0$. Geomorphologically, k_v mapping allows revealing terraces and scarps.

7. Difference curvature (E) is a half-difference of vertical and horizontal curvatures (Shary, 1995)

$$E = \frac{1}{2}(k_v - k_h) = \frac{q^2r - 2pqs + p^2t}{(p^2+q^2)\sqrt{1+p^2+q^2}} - \frac{(1+q^2)r - 2pqs + (1+p^2)t}{2\sqrt{(1+p^2+q^2)^3}} \quad (11)$$

This variable can be positive, negative or zero. The unit of E is m^{-1}. Difference curvature (Figure 3(h)) shows to what extent the relative deceleration of flows (measured by k_v) is higher than flow convergence (measured by k_h) at a given point of the topographic surface.

8. Horizontal excess curvature (k_{he}) is a difference of horizontal and minimal curvatures (Shary, 1995)

$$k_{he} = k_h - k_{\min} = M - E \quad (12)$$

This is a non-negative variable. The unit of k_{he} is m^{-1}. Horizontal excess curvature (Figure 3(i)) shows to what extent the bending of a normal section tangential to a contour line is larger than the minimal bending at a given point of the topographic surface.

9. Vertical excess curvature (k_{ve}) is a difference of vertical and minimal curvatures (Shary, 1995)

$$k_{ve} = k_v - k_{\min} = M + E \quad (13)$$

This is a non-negative variable. The unit of k_{ve} is m^{-1}. Vertical excess curvature (Figure 3(j)) shows to what extent the bending of a normal section having a common tangent line with a slope line is larger than the minimal bending at a given point of the topographic surface.

10. Accumulation curvature (K_a) is a product of vertical and horizontal curvatures (Shary, 1995)

$$K_a = k_h k_v = \frac{(q^2 r - 2pqs + p^2 t)(p^2 r + 2pqs + q^2 t)}{[(p^2 + q^2)(1 + p^2 + q^2)]^2} \quad (14)$$

This variable can be positive, negative or zero. The unit of K_a is m^{-2}. Accumulation curvature (Figure 3(k)) is a measure of the extent of local accumulation of flows at a given point of the topographic surface.

11. Ring curvature (K_r) is a product of horizontal excess and vertical excess curvatures (Shary, 1995)

$$K_r = k_{he} k_{ve} = M^2 - E^2 = \left[\frac{(p^2 - q^2)s - pq(r - t)}{(p^2 + q^2)(1 + p^2 + q^2)}\right]^2 \quad (15)$$

This is a non-negative variable. The unit of K_r is m^{-2}. Ring curvature (Figure 3(l)) describes flow line twisting.

12. Rotor (rot) is a curvature of a flow line (Shary, 1991)

$$rot = \frac{(p^2 - q^2)s - pq(r - t)}{\sqrt{(p^2 + q^2)^3}} \quad (16)$$

This variable can be positive, negative or zero. The unit of rot is m^{-1}. Rotor (Figure 3(m)) describes flow line twisting. A flow line turns clockwise if $rot > 0$, while it turns counter clockwise if $rot < 0$.

13. Horizontal curvature deflection (or generating function) (D_{kh}) is a derivative of k_h by the contour line length (Florinsky, 2009; Shary and Stepanov, 1991)

$$D_{kh} = \frac{q^3 g - p^3 h + 3pq(pm - qk)}{\sqrt{(p^2 + q^2)^3 (1 + p^2 + q^2)}} - k_h rot \frac{2 + 3(p^2 + q^2)}{1 + p^2 + q^2} \quad (17)$$

This variable can be positive, negative or zero. The unit of D_{kh} is m^{-2}. Horizontal curvature deflection (Figure 3(n)) measures the deviation of k_h from loci of the extreme curvature of the topographic surface.

14. Vertical curvature deflection (or tangent change of profile curvature) (D_{kv}) is a derivative of k_v by the contour line length (Jenčo et al., 2009)

$$D_{kv} = \frac{q^3 m - p^3 k + 2pq(qk - pm) - pq(qh - pg)}{\sqrt{(p^2 + q^2)^3 (1 + p^2 + q^2)^3}} - rot \left[\frac{2(r + t)}{\sqrt{(1 + p^2 + q^2)^3}} + k_v \frac{2 + 5(p^2 + q^2)}{(1 + p^2 + q^2)}\right] \quad (18)$$

This variable can be positive, negative or zero. The unit of D_{kv} is m^{-2}. Vertical curvature deflection (Figure 3(o)) measures the deviation of k_v from loci of the extreme curvature of the topographic surface.

4.3 Local morphometric variables: form attributes

1. Minimal curvature (k_{min}) is a curvature of a principal section (Figure 1(a)) with the lowest value of curvature at a given point of the surface (Gauss, 1828; Shary, 1995)

$$k_{\min} = H - M = H - \sqrt{H^2 - K} \quad (19)$$

This variable can be positive, negative or zero. The unit of k_{min} is m^{-1}. Geomorphologically, positive values of minimal curvature (Figure 4(a)) correspond to local convex landforms, while its negative values relate to elongated concave landforms (e.g. troughs and valleys).

2. Maximal curvature (k_{max}) is a curvature of a principal section (Figure 1(a)) with the highest value of curvature at a given

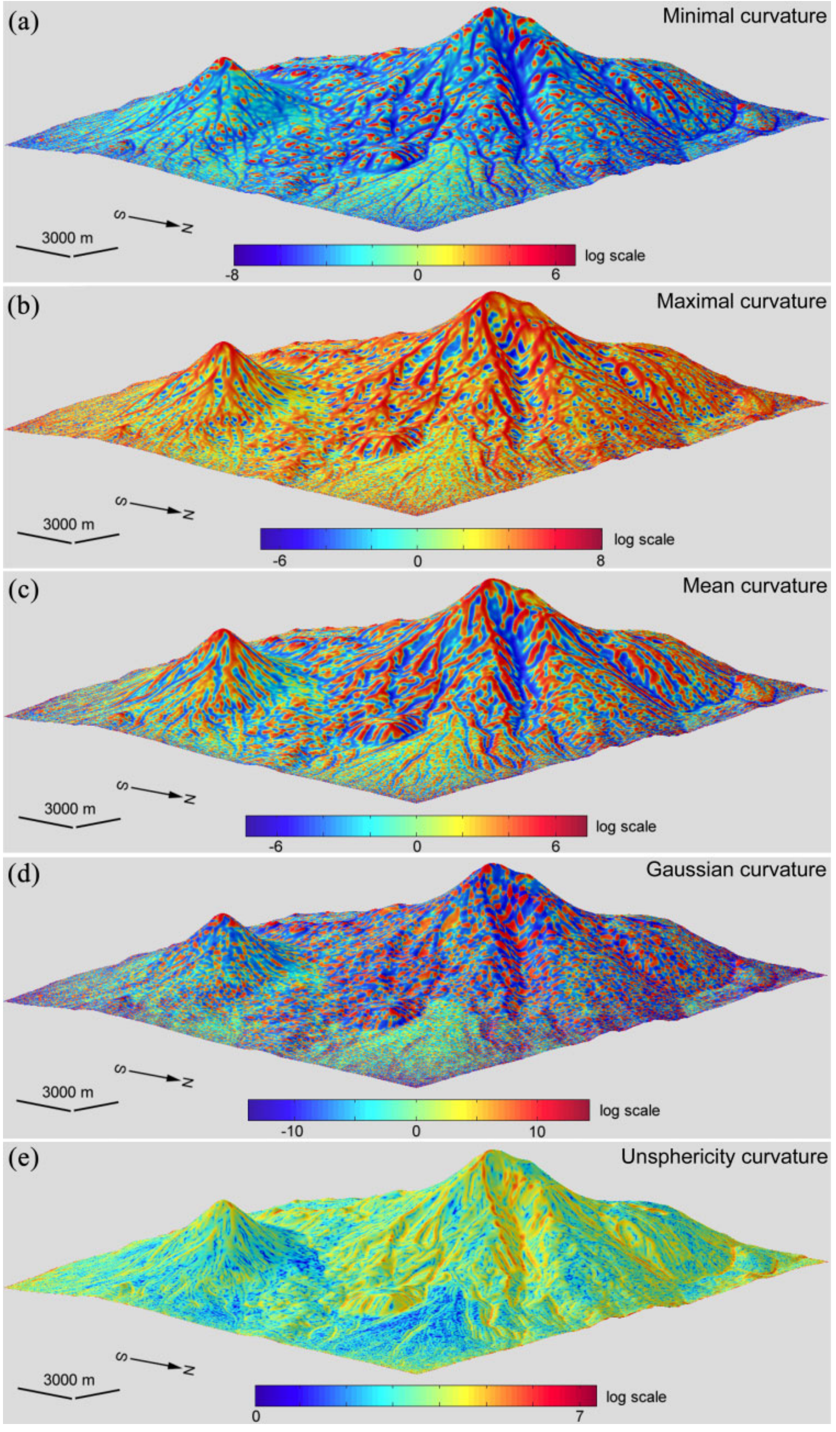

Figure 4. Mount Ararat, local variables, form attributes: (a) minimal curvature; (b) maximal curvature; (c) mean curvature; (d) Gaussian curvature; (e) unsphericity curvature; (f) Laplacian; (g) shape index; (h) curvedness.

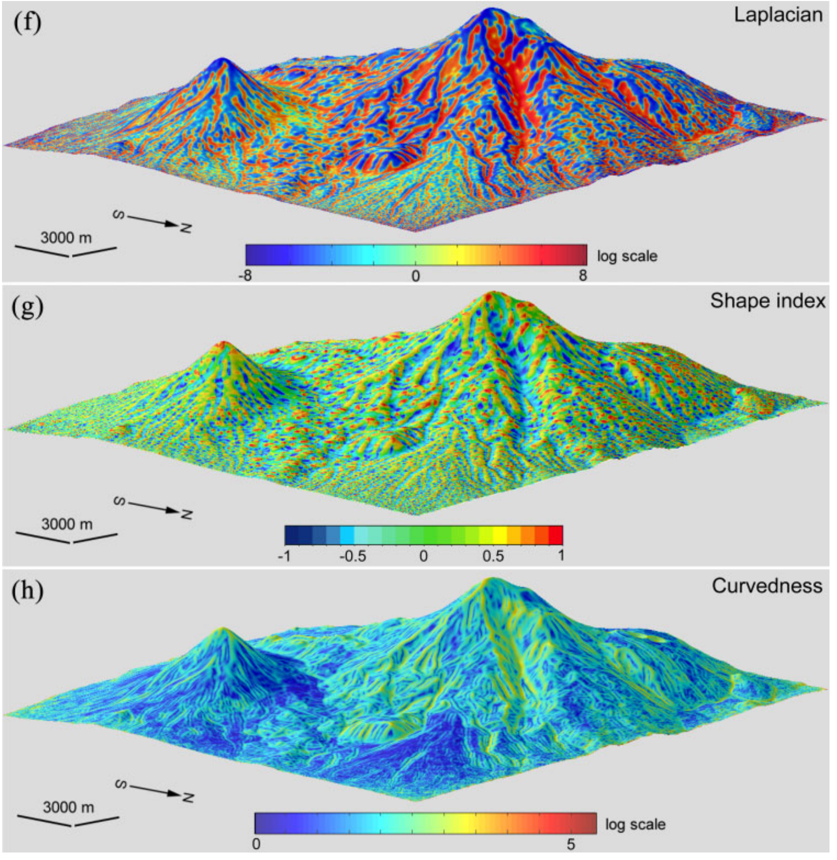

Figure 4. (Continued)

point of the surface (Gauss, 1828; Shary, 1995)

$$k_{\max} = H + M = H + \sqrt{H^2 - K} \quad (20)$$

This variable can be positive, negative or zero. The unit of k_{max} is m^{-1}. Geomorphologically, positive values of maximal curvature (Figure 4(b)) correspond to elongated convex landforms (e.g. ridges), while its negative values relate to local concave landforms.

3. Mean curvature (H) is a half-sum of curvatures of any two orthogonal normal sections at a given point of the topographic surface (Shary, 1991; Young, 1805)

$$H = \frac{1}{2}(k_{\min} + k_{\max}) = \frac{1}{2}(k_h + k_v) = -\frac{(1+q^2)r - 2pqs + (1+p^2)t}{2\sqrt{(1+p^2+q^2)^3}} \quad (21)$$

This variable can be positive, negative or zero. The unit of H is m^{-1}. Mean curvature (Figure 4(c)) represents two accumulation mechanisms of gravity-driven substances – convergence and relative deceleration of flows – with equal weights.

4. Gaussian curvature (K) is a product of maximal and minimal curvatures (Gauss, 1828)

$$K = k_{\min}k_{\max} = \frac{rt - s^2}{(1+p^2+q^2)^2} \quad (22)$$

This variable can be positive, negative or zero. The unit of K is m^{-2}. According to *Teorema egregium*, Gaussian curvature (Figure 4(d)) retains values in each point of the surface after its bending without breaking, stretching and compressing (Gauss, 1828).

5. Unsphericity curvature (M) is a half-difference of maximal and minimal curvatures (Shary, 1995)

$$M = \frac{1}{2}(k_{\max} - k_{\min}) = \sqrt{H^2 - K} = \sqrt{\frac{1}{4(1+p^2+q^2)^3}\left\{\left(r\sqrt{\frac{1+q^2}{1+p^2}} - t\sqrt{\frac{1+p^2}{1+q^2}}\right)^2 (1+p^2+q^2) + \left(pqr\sqrt{\frac{1+q^2}{1+p^2}} - 2s\sqrt{(1+q^2)(1+p^2)} + pqt\sqrt{\frac{1+p^2}{1+q^2}}\right)^2\right\}} \quad (23)$$

This is a non-negative variable. The unit of M is m^{-1}. Unsphericity curvature (Figure 4(e)) shows the extent to which the shape of the surface is non-spherical at a given point.

6. Laplacian (∇^2) is a second-order differential operator, which can be defined as the divergence of the gradient of a function z (Laplace, 1799)

$$\nabla^2 = \text{div grad} = r + t \quad (24)$$

This variable can be positive, negative or zero. The unit of ∇^2 is m^{-1}. Laplacian (Figure 4(f)) measures the flux density of slope lines.

7. Shape index (IS) is a continual form of the discrete Gaussian landform classification (Koenderink and van Doorn, 1992)

$$IS = \frac{2}{\pi}\arctan\left(\frac{k_{\max} + k_{\min}}{k_{\max} - k_{\min}}\right) \quad (25)$$

This is a dimensionless variable ranging from –1 to 1 (Figure 4(g)). Its positive values relate to convex landforms, while its negative ones correspond to concave landforms; its absolute values from 0.5 to 1 are associated with elliptic surfaces (hills and closed depressions), whereas its absolute values from 0 to 0.5 relate to hyperbolic ones (saddles).

8. Curvedness (C) is the root mean square of maximal and minimal curvatures (Koenderink and van Doorn, 1992)

$$C = \sqrt{\frac{k_{\max}^2 + k_{\min}^2}{2}} \quad (26)$$

This is a non-negative variable. The unit of C is m^{-1}. Curvedness (Figure 4(h)) measures the magnitude of surface bending regardless of its shape. Flat areas have low values of C, while areas with sharp bending are marked by high values of C.

4.4 Non-local morphometric variables

1. Catchment area (CA) is an area of a closed figure formed by a contour segment at a given point of the topographic surface and two flow lines coming from upslope to the contour segment ends (Figure 1(c)) (Speight, 1974). This is a non-negative variable. The unit of CA is m^2. The catchment area (Figure 5(a)) is a measure of the contributing area.

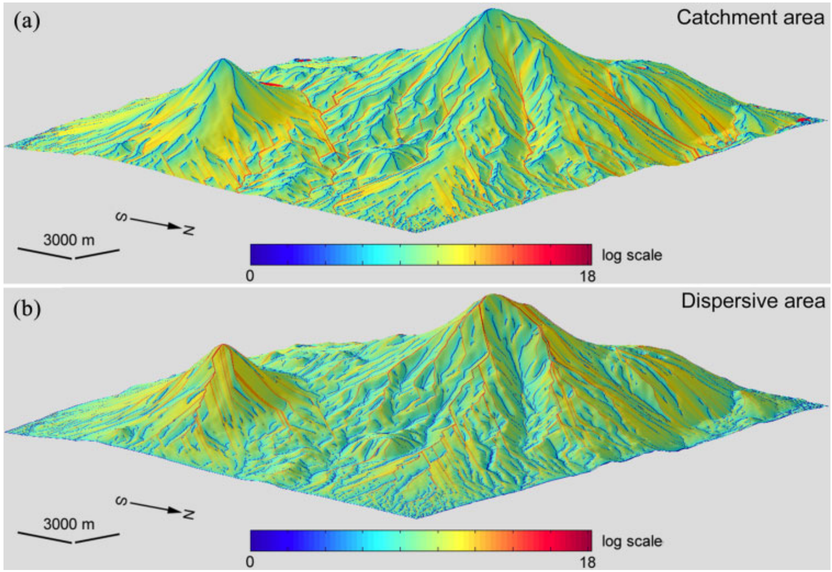

Figure 5. Mount Ararat, non-local variables: (a) catchment area; (b) dispersive area.

2. Dispersive area (*DA*) is an area of a closed figure formed by a contour segment at a given point of the topographic surface and two flow lines going down slope from the contour segment ends (Figure 1(c)) (Speight, 1974). This is a non-negative variable. The unit of *DA* is m^2. The dispersive area (Figure 5(b)) is a measure of a downslope area potentially exposed by flows passing through a given point.

4.5 Two-field specific morphometric variables

1. Reflectance (R) is a measure of the brightness of an illuminated surface (Horn, 1981). For the case of the ideal diffusion (the Lambertian surface)

$$R = \frac{1 - p\sin\theta \operatorname{ctg}\psi - q\cos\theta \operatorname{ctg}\psi}{\sqrt{1+p^2+q^2}\sqrt{1+(\sin\theta \operatorname{ctg}\psi)^2+(\cos\theta \operatorname{ctg}\psi)^2}} \tag{27}$$

where θ and ψ are the solar azimuth and elevation angles (Figure 1(d)), correspondingly.

This is a non-negative dimensionless variable normalized for the range from 0 to 1. Reflectance maps (Figure 6(a)) clearly and plastically display the topography.

2. Insolation (I) is a proportion of maximal direct solar irradiation at the Sun's position determined by solar azimuth and solar elevation (Figure 1(d)) (Shary et al., 2005)

$$I = 50\{1 + \operatorname{sign}[\sin\psi - \cos\psi(p\sin\theta + q\cos\theta)]\} \times \frac{[\sin\psi - \cos\psi(p\sin\theta + q\cos\theta)]}{\sqrt{1+p^2+q^2}} \tag{28}$$

This is a non-negative variable ranging from 0 to 100. The unit of I is per cent. Insolation (Figure 6(b)) characterizes a perpendicularity of the incidence of solar rays on the topographic surface.

4.6 Combined morphometric variables

1. Topographic index (*TI*) is a ratio of catchment area to slope at a given point

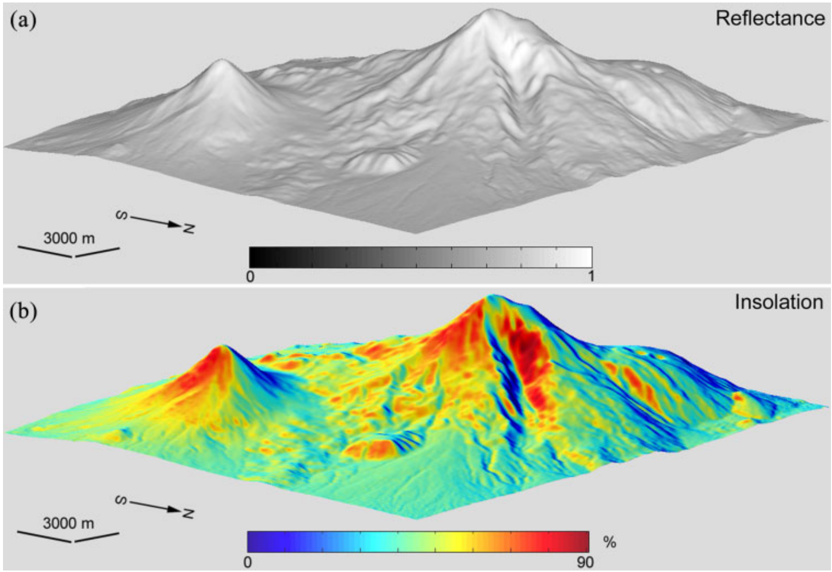

Figure 6. Mount Ararat, two-field specific variables: (a) reflectance (the Lambertian model; $\theta = 45°$; $\psi = 35°$); (b) insolation ($\theta = 90°$; $\psi = 20°$).

of the topographic surface (Beven and Kirkby, 1979)

$$TI = \ln[1 + CA/(10^{-3} + \mathrm{tg}G)] \quad (29)$$

This is a non-negative dimensionless variable. The term 10^{-3} is used to avoid division by zero for the case of horizontal planes. The topographic index (Figure 7(a)) is a measure of the extent of flow accumulation in TOPMODEL, a concept of distributed hydrological modelling (Beven and Kirkby, 1979). *TI* reaches high values in areas with high values of *CA* at low values of *G* (e.g. a terrain with a large upslope contributing area and flat local topography).

2. Stream power index (*SI*) is a product of catchment area and slope at a given point of the topographic surface (Moore et al., 1991)

$$SI = \ln(1 + CA \cdot \mathrm{tg}G) \quad (30)$$

This is a non-negative dimensionless variable. Stream power index (Figure 7(b)) is a measure of potential flow erosion and related landscape processes. *SI* reaches high values in areas with high values of both *CA* and *G* (e.g. a highly sloped terrain with a large upslope contributing area).

V Discussion

5.1 The main paradox of general geomorphometry

It is quite obvious that the real topography is non-smooth and so non-differentiable (Shary, 2008). This means that it cannot have partial derivatives and so local morphometric variables, which are functions of the partial derivatives (sections 4.2 and 4.3). However, introducing the concept of the topographic surface and accepting the condition of its smoothness (section II), we are able not only to calculate local variables, but also to apply these ‘non-existent and abstract’ attributes to study and model relationships between topography and properties of other components of geosystems (for examples, see section 5.2). Topography influences soil and other landscape

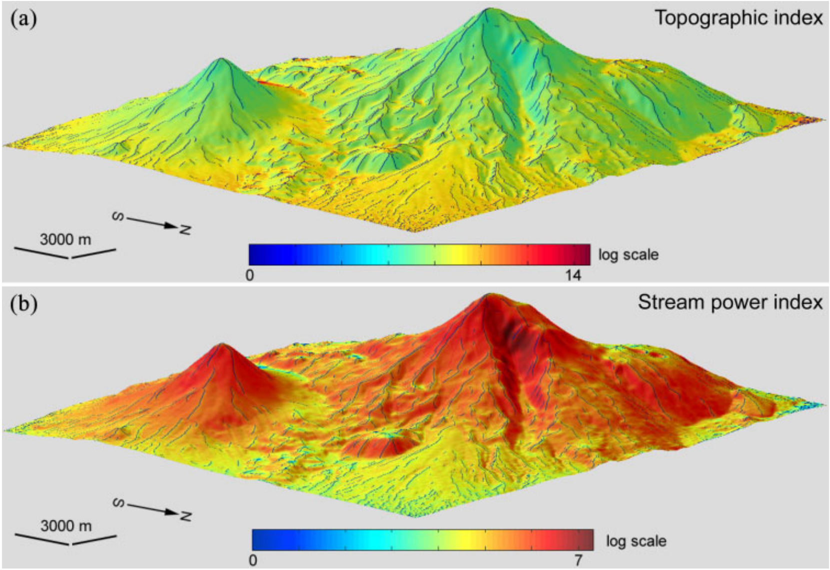

Figure 7. Mount Ararat, combined variables: (a) topographic index; (b) stream power index.

properties mainly via gravity-driven overland and intrasoil lateral migration and accumulation of water. Dependences of soil and other landscape properties on 'non-existent' morphometric attributes may be explained by a hypothetical assumption that real soil hydrological processes also 'smooth' the topography 'ignoring' its minor non-smooth details.

Computationally, the non-smoothness of the real topography is considered in finite-difference methods calculating local variables with 3×3 or 5×5 moving windows (Evans, 1980; Florinsky, 1998c, 2009; Minár et al., 2013; Shary, 1995; Shary et al., 2002). In these algorithms, the smoothness condition of the topographic surface should be met within a moving window only (a polynomial is approximated to 9 or 25 points of a window; there is no approximation between windows). In the same manner, the non-smoothness of the real topography is considered in calculations of its spatial statistical metrics (so-called roughness indices, see section 5.3). Such calculations are also performed with moving windows.

Concepts and methods of fractal geometry (Gao and Xia, 1996; Mandelbrot, 1967) were sometimes applied in general geomorphometry (Klinkenberg, 1992; Mark and Aronson, 1984; McClean and Evans, 2000; Xu et al., 1993). In particular, there were ideas to use fractal dimensions of a terrain as a morphometric index. However, Clarke (1988) clearly demonstrated that a fractal component of topography is important for landscape simulation only. In scientific studies, a fractal component of topography can be considered a high-frequency noise. Thus, we use such a limitation (#5) in the concept of the topographic surface (see section II).

5.2 Application of morphometric variables

Let us briefly consider the application of the reviewed morphometric variables. Slope and aspect have been well known in geosciences for many decades, and so there is no need to specify their fields of application. Curvatures are systematically used in geomorphic studies to describe, analyse and model landforms and their evolution (Burian et al., 2015; Elmahdy and

Mohamed, 2013; Evans, 1980; Guida et al., 2016; Melis et al., 2014; Mitusov et al., 2013, 2014; Prasicek et al., 2014; Temovski and Milevski, 2015). In soil science and ecology, curvatures are regularly applied to study relationships in the topography–soil–vegetation system and to perform predictive soil and vegetation mapping (Behrens et al., 2010; Florinsky et al., 2002; Moore et al., 1993; Omelko et al., 2012; Sharaya and Shary, 2011; Shary and Pinskii, 2013; Shary and Smirnov, 2013; Shary et al., 2016; Stumpf et al., 2017). In structural geology, curvatures are utilized to reveal hidden faults as well as to study fold geometry (Bergbauer, 2007; Florinsky, 1996; Lisle and Toimil, 2007; Mynatt et al., 2007; Roberts, 2001; Stewart and Podolski, 1998). Application of horizontal and vertical curvature deflections may be useful to recognize thalweg and crest lines (Florinsky, 2009; Minár et al., 2013). Reflectance maps are well known in cartography as hill-shaded maps (Jenny, 2001). Insolation is utilized to describe the thermal regime of slopes in geobotanical and agricultural research (Shary and Smirnov, 2013; Shary et al., 2016). Catchment and dispersive areas as well as topographic index are widely used in hydrological and related soil, plant and geomorphic studies (Behrens et al., 2010; Beven, 1997; Florinsky et al., 2002; Mitusov et al., 2013, 2014; Moore et al., 1993; Omelko et al., 2012; Sharaya and Shary, 2011; Shary and Smirnov, 2013). Stream power index is applied in erosion and soil research (Florinsky et al., 2002; Moore et al., 1993; Omelko et al., 2012).

Comprehensive reviews of the application of the morphometric variables can be found elsewhere (Florinsky, 1998b, 2016: pts II and III; Hengl and Reuter, 2009: pt. III; Moore et al., 1991; Wilson and Gallant, 2000).

5.3 Statistical aspects of general geomorphometry

It is clear that some topographic variables can be expressed as linear combinations of others (equations (4)–(30)). For example, mean curvature is a combination of horizontal and vertical curvatures (equation (21)). So, it is not surprising that the results of correlation analysis of models from the complete system of curvatures demonstrate rather high relations between some attributes (Table 2); see, for example, correlation coefficients between k_h and k_{min}, k_{he} and E, k_{max} and H, as well as M and K_r. Thus, questions arise of (1) an information redundancy of the variables discussed in section IV, and (2) the selection of topographic attributes for a particular (e.g. soil) study.

First, although statistical relationships between morphometric variables are useful in geomorphic research (Csillik et al., 2015; Evans, 1980, 1998; Evans and Cox, 1999), such statistics cannot be utilized to select particular variables. Such a selection should be based on their physical/mathematical interpretations. Second, it is a priori impossible to know which particular morphometric variables control, for example, a soil property under given natural conditions. To search topographic attributes controlling the property, it is reasonable to utilize a representative set of the attributes at the first stage of a study (e.g. soil predictive modelling with morphometric variables as predictors; Florinsky, 2016: ch 11; McBratney et al., 2003). When governing variables are found by a correlation analysis, one can reduce their number because it is incorrect to use together, for instance, horizontal, vertical and mean curvatures in a predictive (e.g. regression) model of the property (Florinsky, 2016: 309–311; Shary and Pinskii, 2013).

To delineate and quantitatively describe terrains of different morphologic structure as well as geological composition and age, digital models and maps of topographic (or surface) roughness are used in geomorphic, geological and planetary studies (Fa et al., 2016; Frankel and Dolan, 2007; Grohmann et al., 2011; Herzfeld and Higginson, 1996; Karachevtseva et al., 2015; Kreslavsky and Head, 2000; McKean and

Roering, 2004; Trevisani and Rocca, 2015). To avoid confusion, we should stress that topographic roughness is not a morphometric variable. It is a generalized term, without a clear definition, which is usually applied to denote some spatial statistical metrics of a morphometric model (e.g. median absolute value of slope, eigenvalue ratios of external normals, standard deviation of elevation, slope, etc.). Models of topographic roughness are usually calculated using windows moving along a morphometric model. The principal difference between morphometric variables and topographic roughness is as follows: Morphometric variables mathematically describe 'geometry' of the topographic surface and its physically interpretable relationships with other components of geosystems, while topographic roughness statistically describes 'spatial variability' of a particular morphometric property of the topographic surface in the vicinity of a given point of the surface.

5.4 Some pending problems of general geomorphometry

Advances in the terrestrial light detection and ranging (LiDAR) technology (Hodgetts, 2013) have allowed the production of 3D high-resolution models of caves and grottos. Some researchers try to use geomorphometric modelling to analyse the geometry of inner surfaces of these objects (Brook et al., 2017; Gallay et al., 2015, 2016). However, such an application of geomorphometry violates the limitation #1 stating that the topographic surface is uniquely defined by a single-valued function (see section II). It is obvious that caves and grottos cannot be directly described by a single-valued elevation function because, at least, two values of elevation correspond to a pair of planimetric coordinates.

One may ignore this limitation working with form attributes (e.g. Gallay et al., 2015, 2016), which are gravity field invariants (see section 3.2). However, the limitation becomes important if one works with flow attributes because these are gravity-field specific variables (section 3.2). In water dynamics/runoff on cave ceilings and walls, forces of surface tension can play a dominant role, rather than gravity-driven overland lateral transport of liquids controlled by horizontal and vertical curvatures (section 4.2). This calls into question the adequacy of utilizing these morphometric variables (e.g. Brook et al., 2017) to study hydrological processes in caves, grottos and niches, at least for microtopography of ceilings. This problem requires in-depth study and development of recommendations for geomorphometric modelling in speleology and related disciplines.

There are three other interrelated pending problems.

(1) A set of the third-order local variables was introduced by Jenčo et al. (2009). In general, these attributes describe deviations of the second-order variables from loci of the extreme curvature of the topographic surface (Florinsky, 2009; Minár et al., 2013; Shary and Stepanov, 1991). Only two of them have been discussed here, horizontal and vertical curvature deflections (section 4.2), because their interpretation and practical application are more or less clear: their zero values correlate with crest and thalweg lines. Other third-order variables are still insufficiently studied.

(2) Comparing with the theory of local variables (Jenčo et al., 2009; Shary, 1995), a mathematical theory for non-local attributes is still little developed (Gallant and Hutchinson, 2011; Koshel and Entin, 2017; Orlandini et al., 2014; Peckham, 2013). In particular, Gallant and Hutchinson (2011) proposed a differential equation for calculating specific catchment area. However, a general analytical theory of non-local morphometric variables still does not

exist. The diversity of flow routing algorithms for calculating non-local variables (section 3.3) is a result of underdevelopment of an appropriate mathematical theory.

(3) Loci of extreme curvature of the topographic surface may define four types of structural lines: crests (or ridges), thalwegs (or courses), as well as top and bottom edges (or breaks) of slopes. Although structural lines have been mathematically studied for many decades, an analytical solution based on local differential geometric criteria has not yet been found (see reviews: Koenderink and van Doorn, 1993, 1994). At the same time, crests and thalwegs can be considered as two topologically connected tree-like hierarchical structures (Clarke and Romero, 2017). Maxwell (1870) defined a ridge as a slope line connecting a sequence of local maximal and saddle points, and a thalweg as a slope line connecting a sequence of local minimal and saddle points. Rothe (1915) argued that crests and thalwegs are singular solutions of the differential equation of the slope lines. Koenderink and van Doorn (1993) supposed that crests and thalwegs are the special type of slope lines where other ones converge, and they also argued that local differential geometric criteria for crests and thalwegs cannot exist. Since the problem of analytical description of structural lines has not been resolved, practical derivation of crests and thalwegs is mainly carried out by flow routing algorithms, similar to calculations of non-local variables (see reviews: Clarke and Romero, 2017; López et al., 1999; Tribe, 1992). Hopefully, these three interrelated problems will be solved in the near future.

Existing algorithms of geomorphometry can be applied to DEMs given on plane square grids (Evans, 1980; Florinsky, 2009; Freeman, 1991; Martz and de Jong, 1988; Minár et al., 2013; Quinn et al., 1991; Shary, 1995; Tarboton, 1997; Zevenbergen and Thorne, 1987) as well as spheroidal equal angular grids located on an ellipsoid of revolution and a sphere (Florinsky, 1998c, 2017a). Geomorphometric computations on spheroidal equal angular grids are trivial for the Earth, Mars, the Moon, Venus and Mercury (Florinsky, 2008a, 2008b; Florinsky and Filippov, 2017; Florinsky et al., 2017a). This is because forms of the above mentioned celestial bodies can be described by an ellipsoid of revolution or a sphere. For these surfaces, there are well-developed theory and computational algorithms to solve the inverse geodetic problem (Bagratuni, 1967; Bessel, 1825; Karney, 2013; Morozov, 1979; Sjöberg, 2006; Vincenty, 1975). Formulae for the solution of this problem are used to determine parameters of moving windows in morphometric calculations (Florinsky, 2017a). At the same time, it is advisable to apply a triaxial ellipsoid for describing forms of small moons and asteroids (Bugaevsky, 1999; Stooke, 1998; Thomas, 1989). However, for the case of a triaxial ellipsoid, solutions of the inverse geodetic problem are presented in general form only (Bespalov, 1980; Jacobi, 1839; Karney, 2012; Krasovsky, 1902; Panou, 2013; Shebuev, 1896). This makes difficult geomorphometric modelling of small moons and asteroids. Thus, the next item on the geomorphometric agenda is development of computational algorithms for modelling on a surface of a triaxial ellipsoid (Florinsky, 2017b).

VI Conclusions

In the last 25 years, great progress has been made in the field of geomorphometry.

(1) A physical and mathematical theory of the topographic surface has substantially evolved (Evans, 1972, 1980; Gallant and Hutchinson, 2011; Jenčo, 1992; Jenčo et al., 2009; Koenderink and van Doorn, 1992, 1994; Krcho, 1973, 2001; Shary, 1991, 1995; Shary et al., 2002, 2005).

(2) Effective algorithms for calculating attributes from DEMs have been developed (Evans, 1980; Florinsky, 1998c, 2009; Florinsky and Pankratov, 2016; Freeman, 1991; Martz and de Jong, 1988; Minár et al., 2013; Shary, 1995; Tarboton, 1997).

(3) High- and super high-resolution DEMs have become widely available (Tarolli, 2014) owing to advances in LiDAR technology (Liu, 2008), real-time kinematic global navigation satellite system (GNSS) surveys (Awange, 2012: ch 8), areal surveys based on unmanned aerial vehicles (UAVs) (Colomina and Molina, 2014), and structure-from-motion (SfM) techniques (Smith et al., 2016). UAVs and SfM introduce a low-cost alternative to manned aerial surveys and conventional photogrammetry. UAV/SfM-derived, photogrammetrically sound DEMs can be successfully used for further geomorphometric modelling: it is possible to produce noiseless, well-readable and interpretable models of slope and curvatures (with the resolution of 5–20 cm) for grassy areas with separately standing groups of trees, shrubs and other objects (Florinsky et al., 2017b).

(4) Quasi-global and global, medium- and high-resolution DEMs of the Earth (SRTM1 (Farr et al., 2007), Advanced Spaceborne Thermal Emission and Reflection Radiometer Global DEM (ASTER GDEM) (Toutin, 2008), SRTM30_PLUS (Becker et al., 2009), SRTM15_PLUS (Olson et al., 2014), WorldDEM (Zink et al., 2014) and Advanced Land Observing Satellite World 3D model (ALOS World 3D) (Tadono et al., 2014)) have been produced and become available.

(5) There are new bathymetric DEMs (Arndt et al., 2013; Jakobsson et al., 2012; Weatherall et al., 2014). Submarine topography influences ocean currents, distribution of perennial ice and sediment migration. Submarine valleys participate in the gravity-driven transport of substances from land to ocean. Geomorphometric modelling of submarine topography can provide new opportunities for oceanological, marine geomorphological and marine geological studies.

(6) There are new DEMs for the ice bed topography of Greenland (Bamber et al., 2013) and Antarctica (Fretwell et al., 2013). In this case, application of geomorphometric methods can produce new results for understanding both glaciological processes and geological structure of glacier-covered terrains.

(7) Advances in 3D seismic surveys offer a wide field of activity in applying principles of geomorphometric modelling to subterranean surfaces (Chopra and Marfurt, 2007) that can give a new impetus to geological research.

(8) Global, extra-terrestrial medium-resolution DEMs for Mars (Smith et al., 1999), the Moon (Smith et al., 2010), Phobos (Karachevtseva et al., 2014) and Mercury (Becker et al., 2016) are available. Geomorphometry can provide additional tools for comparative planetary studies.

(9) Morphometric globes for the Earth, Mars and the Moon have been developed (Florinsky and Filippov, 2017; Florinsky et al., 2017a) owing to advances in scientific visualization (Hansen and Johnson, 2005) and virtual globe (Cozzi and Ring, 2011) technologies. Such virtual globes can be easily utilized by users without special training in geomorphometry.

The above achievements and future possibilities, as well as reproducibility, relative simplicity and flexibility of geomorphometric methods, determine their potential for geosciences. It should be realized, however, that the governing factor for the evolution of digital terrain analysis is advances in the theory of the topographic surface, which lays a rigorous physical and mathematical foundation for both computation algorithms and applied issues of topographic modelling.

Acknowledgements

The author is grateful to Ian Evans and two anonymous reviewers for constructive criticism.

Declaration of Conflicting Interests

The author declared no potential conflicts of interest with respect to the research, authorship, and/or publication of this article.

Funding

The author disclosed receipt of the following financial support for the research, authorship, and/or publication of this article: This study was supported by the Russian Foundation for Basic Research, Grant number 15-07-02484.

Notes

1. A slope line is a space curve on the topographic surface. At each point of the curve, the direction of the tangent to the curve coincides with the direction of the tangential component of the gravitational force (Cayley, 1859).
2. A flow line is a plane curve, a projection of a slope line to a horizontal plane.

References

Aandahl AR (1948) The characterization of slope positions and their influence on the total nitrogen content of a few virgin soils of western Iowa. *Soil Science Society of America Proceedings* 13: 449–454.

Arndt JE, Schenke HW, Jakobsson M, et al. (2013) The International Bathymetric Chart of the Southern Ocean (IBCSO) Version 1.0: A new bathymetric compilation covering circum-Antarctic waters. *Geophysical Research Letters* 40: 3111–3117.

Awange JL (2012) *Environmental Monitoring Using GNSS: Global navigation satellite systems*. Berlin: Springer.

Bagratuni GV (1967) *Course in Spheroidal Geodesy*. Wright-Patterson, OH: Foreign Technology Division.

Bamber JL, Griggs JA, Hurkmans RTWL, et al. (2013) A new bed elevation data-set for Greenland. *Cryosphere* 7: 499–510.

Becker JJ, Sandwell DT, Smith WHF, et al. (2009) Global bathymetry and elevation data at 30 arc seconds resolution: SRTM30_PLUS. *Marine Geodesy* 32: 355–371.

Becker KJ, Robinson MS, Becker TL, et al. (2016) First global digital elevation model of Mercury. In: *47th Lunar and Planetary Science Conference*, 21–25 March 2016, Woodlands, Texas. Houston, TX: Lunar and Planetary Institute: # 2959.

Behrens T, Zhu AX, Schmidt K, et al. (2010) Multi-scale digital terrain analysis and feature selection for digital soil mapping. *Geoderma* 155: 175–185.

Bergbauer S (2007) Testing the predictive capability of curvature analyses. *Geological Society of London Special Publications* 292: 185–202.

Bespalov NA (1980) *Methods for Solving Problems of Spheroidal Geodesy*. Moscow: Nedra (in Russian).

Bessel FW (1825) Über die Berechnung der geographischen Längen und Breiten aus geodätischen Vermessungen. *Astronomische Nachrichten* 4: 241–254.

Beven K (1997) TOPMODEL: A critique. *Hydrological Processes* 11: 1069–1085.

Beven KJ and Kirkby MJ (1979) A physically-based variable contributing area model of basin hydrology. *Hydrological Science Bulletin* 24: 43–69.

Brocklehurst SH (2010) Tectonics and geomorphology. *Progress in Physical Geography* 34: 357–383.

Brook A, Ben-Binyamin A and Shtober-Zisu N (2017) Inland notches micromorphology. *Geophysical Research Abstracts* 19: EGU2017–1289.

Bugaevsky LM (1999) *Theory of Cartographic Projections of Regular Surfaces*. Moscow: Zlatoust (in Russian).

Burbank DW and Anderson RS (2012) *Tectonic Geomorphology*, 2nd edn. Chichester, UK: Wiley Blackwell.

Burian L, Mitusov AV and Poesen J (2015) Relationships of attributes of gullies with morphometric variables. In: Jasiewicz J, Zwoliński Z, Mitasova H, et al. (eds) *Geomorphometry for Geosciences*. Poznań, Poland: Institute of Geoecology and Geoinformation, 111–114.

Burrough PA (1986) *Principles of Geographical Information Systems for Land Resources Assessment*. Oxford: Clarendon Press.

Cayley A (1859) On contour and slope lines. *The London, Edinburgh and Dublin Philosophical Magazine and Journal of Science Ser* 4 18: 264–268.

Chopra S and Marfurt KJ (2007) *Seismic Attributes for Prospect Identification and Reservoir Characterization*. Tulsa, OK: Society of Exploration Geophysicists.

Clarke JI (1966) Morphometry from maps. In: Dury GH (ed) *Essays in Geomorphology*. London: Heinemann, 235–274.

Clarke KC (1988) Scale-based simulation of topographic relief. *American Cartographer* 15: 173–181.

Clarke KC and Romero BE (2017) On the topology of topography: A review. *Cartography and Geographic Information Science* 44: 271–282.

Colomina I and Molina P (2014) Unmanned aerial systems for photogrammetry and remote sensing: A review. *ISPRS Journal of Photogrammetry and Remote Sensing* 92: 79–97.

Cozzi P and Ring K (2011) *3D Engine Design for Virtual Globes*. Boca Raton, FL: A K Peters and CRC Press.

Csillik O, Evans IS and Drăguţ L (2015) Transformation (normalization) of slope gradient and surface curvatures, automated for statistical analyses from DEMs. *Geomorphology* 232: 65–77.

Deng Y (2007) New trends in digital terrain analysis: Landform definition, representation and classification. *Progress in Physical Geography* 31: 405–419.

Dikau R (1988) Case studies in the development of derived geomorphic maps. *Geologisches Jahrbuch* A104: 329–338.

Elmahdy SI and Mohamed MM (2013) Remote sensing and GIS applications of surface and near-surface hydromorphological features in Darfur region, Sudan. *International Journal of Remote Sensing* 34: 4715–4735.

Ettema CH and Wardle DA (2002) Spatial soil ecology. *Trends in Ecology and Evolution* 17: 177–183.

Evans IS (1972) General geomorphometry, derivations of altitude and descriptive statistics. In: Chorley RJ (ed) *Spatial Analysis in Geomorphology*. London: Methuen.

Evans IS (1979) Statistical characterization of altitude matrices by computer: An integrated system of terrain analysis and slope mapping. The final report on grant DA-ERO-591-73-G0040. Durham, UK: University of Durham.

Evans IS (1980) An integrated system of terrain analysis and slope mapping. *Zeitschrift für Geomorphologie* Suppl. 36: 274–295.

Evans IS (1998) What do terrain statistics really mean? In: Lane SN, Richards KS and Chandler JH (eds) *Landform Monitoring, Modelling and Analysis*. Chichester, UK: J Wiley & Son, 119–138.

Evans IS and Cox NJ (1999) Relations between land surface properties: Altitude, slope and curvature. *Lecture Notes in Earth Sciences* 78: 13–45.

Evans IS and Minár J (2011) A classification of geomorphometric variables. In: Hengl T, Evans IS, Wilson JP, et al. (eds) *Proceedings of Geomorphometry 2011*, Redlands, CA, 7–11 September 2011, 105–108. International Society for Geomorphometry.

Fa W, Cai Y, Xiao Z, et al. (2016) Topographic roughness of the northern high latitudes of Mercury from MESSENGER Laser Altimeter data. *Geophysical Research Letters* 43: 3078–3087.

Farr TG, Rosen PA and Caro E, et al. (2007) The Shuttle Radar Topography Mission. *Reviews of Geophysics* 45: RG2004.

Fisher PF (1996) Extending the applicability of viewsheds in landscape planning. *Photogrammetric Engineering and Remote Sensing* 62: 1297–1302.

Florinsky IV (1996) Quantitative topographic method of fault morphology recognition. *Geomorphology* 16: 103–119.

Florinsky IV (1998a) Accuracy of local topographic variables derived from digital elevation models. *International Journal of Geographical Information Science* 12: 47–61.

Florinsky IV (1998b) Combined analysis of digital terrain models and remotely sensed data in landscape investigations. *Progress in Physical Geography* 22: 33–60.

Florinsky IV (1998c) Derivation of topographic variables from a digital elevation model given by a spheroidal trapezoidal grid. *International Journal of Geographical Information Science* 12: 829–852.

Florinsky IV (2008a) Global lineaments: Application of digital terrain modelling. In: Zhou Q, Lees B and Tang G-A (eds) *Advances in Digital Terrain Analysis*. Berlin: Springer, 365–382.

Florinsky IV (2008b) Global morphometric maps of Mars, Venus and the Moon. In: Moore A and Drecki I (eds) *Geospatial Vision: New dimensions in cartography*. Berlin: Springer, 171–192.

Florinsky IV (2009) Computation of the third-order partial derivatives from a digital elevation model. *International Journal of Geographical Information Science* 23: 213–231.

Florinsky IV (2016) *Digital Terrain Analysis in Soil Science and Geology*, 2nd edn. Amsterdam: Academic Press.

Florinsky IV (2017a) Spheroidal equal angular DEMs: The specifity of morphometric treatment. *Transactions in GIS* 21. Epub ahead of print 15 February 2017. DOI:10.1111/tgis.12269.

Florinsky IV (2017b) Towards geomorphometric modelling on a surface of a triaxial ellipsoid (formulation of the problem). In: Tikunov VS (ed) *InterCarto/InterGIS 23: Geoinformation Support of Sustainable Development of Territories in the Context of Global Climate Change: Proceedings of the International Conference,* Yuzhno-Sakhalinsk, Russia, 26–28 June 2017, Vol 2, 130–143. Moscow: Moscow University Press, 130–143 (in Russian, with English abstract).

Florinsky IV and Filippov SV (2017) A desktop system of virtual morphometric globes for Mars and the Moon. *Planetary and Space Science* 137: 32–39.

Florinsky IV and Pankratov AN (2016) A universal spectral analytical method for digital terrain modeling. *International Journal of Geographical Information Science* 30: 2506–2528.

Florinsky IV, Eilers RG, Manning G, et al. (2002) Prediction of soil properties by digital terrain modelling. *Environmental Modelling and Software* 17: 295–311.

Florinsky I, Garov A and Karachevtseva I (2017a) A web-system of virtual morphometric globes. *Geophysical Research Abstracts* 19: EGU2017–99.

Florinsky IV, Kurkov VM and Bliakharskii DP (2017b) Geomorphometry from unmanned aerial surveys. *Transactions in GIS* 21. Epub ahead of print 20 September 2017. DOI: 10.1111/tgis.12296.

Frankel KL and Dolan JF (2007) Characterizing arid-region alluvial fan surface roughness with airborne laser swath mapping digital topographic data. *Journal of Geophysical Research* 112: F02025.

Franklin J (1995) Predictive vegetation mapping: Geographic modelling of biospatial patterns in relation to environmental gradients. *Progress in Physical Geography* 19: 474–499.

Freeman TG (1991) Calculating catchment area with divergent flow based on a regular grid. *Computers and Geosciences* 17: 413–422.

Fretwell P, Pritchard HD, Vaughan DG, et al. (2013) Bedmap2: Improved ice bed, surface and thickness datasets for Antarctica. *Cryosphere* 7: 375–393.

Gallant JC and Hutchinson MF (2011) A differential equation for specific catchment area. *Water Resources Research* 47: W05535.

Gallay M, Hochmuth Z, Kaňuk J, et al. (2016) Geomorphometric analysis of cave ceiling channels mapped with 3D terrestrial laser scanning. *Hydrology and Earth System Sciences* 20: 1827–1849.

Gallay M, Kaňuk J, Hofierka J, et al. (2015) Mapping and geomorphometric analysis of 3D cave surfaces: A case study of the Domica Cave, Slovakia. In: Jasiewicz J, Zwoliński Z and Mitášová H, et al. (eds) *Geomorphometry for Geosciences*. Poznań, Poland: Institute of Geoecology and Geoinformation, 69–73.

Gao J and Xia Z-G (1996) Fractals in physical geography. *Progress in Physical Geography* 20: 178–191.

Gardiner V and Park CC (1978) Drainage basin morphometry: Review and assessment. *Progress in Physical Geography* 2: 1–35.

Gauss CF (1828) Disquisitiones generales circa superficies curvas. *Commentationes Societatis Regiae Scientiarum Gottingensis Recentiores* 6: 99–146.

Geiger R (1966) *The Climate near the Ground*. Cambridge, MA: Harvard University Press.

Gerrard AJ (1981) *Soils and Landforms: An integration of geomorphology and pedology*. London: George Allen and Unwin.

Grohmann CH, Smith MJ and Riccomini C (2011) Multiscale analysis of topographic surface roughness in the Midland Valley, Scotland. *IEEE Transactions on Geoscience and Remote Sensing* 49: 1200–1213.

Guida D, Cuomo A and Palmieri V (2016) Using object-based geomorphometry for hydro-geomorphological analysis in a Mediterranean research catchment. *Hydrology and Earth System Sciences* 20: 3493–3509.

Hansen CD and Johnson CR (eds) (2005) *The Visualization Handbook*. Amsterdam: Academic Press.

Hengl T and Reuter HI (eds) (2009) *Geomorphometry: Concepts, software, applications*. Amsterdam: Elsevier.

Herzfeld UC and Higginson CA (1996) Automated geostatistical seafloor classification: Principles, parameters, feature vectors and discrimination criteria. *Computers and Geosciences* 22: 35–52.

Hodgetts D (2013) Laser scanning and digital outcrop geology in the petroleum industry: A review. *Marine and Petroleum Geology* 46: 335–354.

Horn BKP (1981) Hill shading and the reflectance map. *Proceedings of the IEEE* 69: 14–47.

Horton RE (1945) Erosional development of streams and their drainage basins: Hydrophysical approach to quantitative morphology. *Geological Society of America Bulletin* 56: 275–370.

Huang P-C and Lee KT (2016) Distinctions of geomorphological properties caused by different flow-direction predictions from digital elevation models. *International Journal of Geographical Information Science* 30: 168–185.

Jacobi CGJ (1839) Note von der geodätischen Linie auf einem Ellipsoid und den verschiedenen Anwendungen einer merkwürdigen analytischen Substitution. *Crelle's Journal für die reine und angewandte Mathematik* 19: 309–313.

Jakobsson M, Mayer L, Coakley B, et al. (2012) The International Bathymetric Chart of the Arctic Ocean (IBCAO) Version 3.0. *Geophysical Research Letters* 39: L12609.

Jenčo M (1992) The morphometric analysis of georelief in terms of a theoretical conception of the complex digital model of georelief. *Acta Facultatis Rerum Naturalium Universitatis Comenianae, Geographica* 33: 133–151.

Jenčo M, Pacina J and Shary PA (2009) Terrain skeleton and local morphometric variables: Geosciences and computer vision technique. In: Horák J, Halounová L, Kusendová D, et al. (eds) *Advances in Geoinformation Technologies 2009*. Ostrava, Czechia: VSB-Technical University of Ostrava, 57–76.

Jenny B (2001) An interactive approach to analytical relief shading. *Cartographica* 38: 67–75.

Jenson SK and Domingue JQ (1988) Extracting topographic structure from digital elevation data for geographic information system analysis. *Photogrammetric Engineering and Remote Sensing* 54: 1593–1600.

Jordan G (2007) Digital terrain analysis in a GIS environment: Concepts and development. In: Peckham RJ and Jordan G (eds) *Digital Terrain Modelling: Development and applications in a policy support environment*. Berlin: Springer, 1–43.

Karachevtseva IP, Kokhanov AA, Konopikhin AA, et al. (2015) Cartographic and geodetic methods to characterize the potential landing sites for the future Russian missions Luna-Glob and Luna-Resurs. *Solar System Research* 49: 92–109.

Karachevtseva IP, Oberst J, Zubarev AE, et al. (2014) The Phobos information system. *Planetary and Space Science* 102: 74–85.

Karney CFF (2012) Geodesics on a triaxial ellipsoid. *GeographicLib* 1.47. Available at: http://geographiclib.sourceforge.net/html/triaxial.html (accessed 13 September 2017).

Karney CFF (2013) Algorithms for geodesics. *Journal of Geodesy* 87: 43–55.

Kirkby MJ and Chorley RJ (1967) Throughflow, overland flow and erosion. *Bulletin of the International Association of Scientific Hydrology* 12: 5–21.

Klinkenberg B (1992) Fractals and morphometric measures: Is there a relationship? *Geomorphology* 5: 5–20.

Koenderink JJ and van Doorn AJ (1992) Surface shape and curvature scales. *Image and Vision Computing* 10: 557–565.

Koenderink JJ and van Doorn AJ (1993) Local features of smooth shapes: Ridges and courses. *Proceedings of SPIE* 2013: 2–13.

Koenderink JJ and van Doorn AJ (1994) Two-plus-one-dimensional differential geometry. *Pattern Recognition Letters* 15: 439–443.

Koshel SM and Entin AL (2017) Catchment area derivation from gridded digital elevation models using the flowline-tracing approach. *Moscow University Bulletin*, *Ser. Geography No*. 3: 42–50 (in Russian).

Krasovsky FN (1902) Determination of the size of the Earth triaxial ellipsoid from the results of the Russian arc measurements. *In: Memorial Book of the Konstantinovsky Mezhevoy Institute for the 1900–1901 years*. Moscow: Russian Association of Printing and Publishing, 19–54 (in Russian).

Kreslavsky MA and Head JW (2000) Kilometer-scale roughness of Mars: Results from MOLA data analysis. *Journal of Geophysical Research* 105(E11): 26,695–26,711.

Krcho J (1973) Morphometric analysis of relief on the basis of geometric aspect of field theory. *Acta Geographica Universitatis Comenianae. Geographico-Physica* 1: 7–233.

Krcho J (1983) Teoretická koncepcia a interdisciplinárne aplikácie komplexného digitálneho modelu reliéfu pri modelovaní dvojdimenzionálnych polí. *Geografický Časopis* 35: 265–291.

Krcho J (2001) *Modelling of Georelief and its Geometrical Structure using DTM: Positional and numerical accuracy*. Bratislava, Slovakia: Q111 Publishers.

Laplace PS (1799) *Traité de Mécanique Céleste,* vol 1. Paris: Duprat.

Lastochkin AN (1987) *Morphodynamical Analysis*. Leningrad: Nedra (in Russian).

Lecours V, Dolan MFJ, Micallef A, et al. (2016) A review of marine geomorphometry, the quantitative study of the seafloor. *Hydrology and Earth System Sciences* 20: 3207–3244.

Li Z, Zhu Q and Gold C (2005) *Digital Terrain Modeling: Principles and methodology*. New York: CRC Press.

Lisle RJ and Toimil NC (2007) Defining folds on three-dimensional surfaces. *Geology* 35: 519–522.

Liu X (2008) Airborne LiDAR for DEM generation: Some critical issues. *Progress in Physical Geography* 32: 31–49.

López AM, Lumbreras F, Serrat J, et al. (1999) Evaluation of methods for ridge and valley detection. *IEEE Transactions on Pattern Analysis and Machine Intelligence* 21: 327–335.

McBratney AB, Mendonça Santos ML and Minasny B (2003) On digital soil mapping. *Geoderma* 117: 3–52.

McClean CJ and Evans IS (2000) Apparent fractal dimensions from continental scale digital elevation models using variogram methods. *Transactions in GIS* 4: 361–378.

McKean J and Roering J (2004) Objective landslide detection and surface morphology mapping using high-resolution airborne laser altimetry. *Geomorphology* 57: 331–351.

Mandelbrot B (1967) How long is the coast of Britain? Statistical self-similarity and fractional dimension. *Science* 156: 636–638.

Mardia KV (1972) *Statistics of Directional Data*. London: Academic Press.

Mark DM (1975) Geomorphometric parameters: A review and evaluation. *Geografiska Annaler, Series A: Physical Geography* 57: 165–177.

Mark DM and Aronson PB (1984) Scale-dependent fractal dimensions of topographic surfaces: An empirical investigation, with applications in geomorphology and computer mapping. *Mathematical Geology* 16: 671–683.

Martz LW and de Jong E (1988) CATCH: a Fortran program for measuring catchment area from digital elevation models. *Computers and Geosciences* 14: 627–640.

Maxwell JC (1870) On hills and dales. *The London, Edinburgh and Dublin Philosophical Magazine and Journal of Science Series* 4 40: 421–427.

Melis MT, Mundula F, Dessì F, et al. (2014) Tracing the boundaries of Cenozoic volcanic edifices from Sardinia (Italy): A geomorphometric contribution. *Earth Surface Dynamics* 2: 481–492.

Miller CL and Leflamme RA (1958) The digital terrain model: Theory and application. *Photogrammetric Engineering* 24: 433–442.

Minár J, Jenčo M, Pacina J, et al. (2013) Third-order geomorphometric variables (derivatives): Definition, computation and utilization of changes of curvatures. *International Journal of Geographical Information Science* 27: 1381–1402.

Minár J, Krcho J and Evans IS (2016) Geomorphometry: Quantitative land-surface analysis. *Reference Module in Earth Systems and Environmental Sciences*. Epub ahead of print 19 August 2016. DOI: 10.1016/B978-0-12-409548-9.10260-X.

Mitášová H and Mitáš L (1993) Interpolation by regularized spline with tension: I. Theory and implementation. *Mathematical Geology* 25: 641–655.

Mitusov AV, Dreibrodt S, Mitusova OE, et al. (2013) Detection of land surface memory by correlations between thickness of colluvial deposits and morphometric variables. *Geomorphology* 191: 109–117.

Mitusov AV, Mitusova OE, Wendt J, et al. (2014) Correlation of colluvial deposits with the modern land surface and the problem of slope profile description. *Geomorphology* 220: 30–40.

Moore ID, Gessler PE, Nielsen GA, et al. (1993) Soil attribute prediction using terrain analysis. *Soil Science Society of America Journal* 57: 443–452.

Moore ID, Grayson RB and Ladson AR (1991) Digital terrain modelling: A review of hydrological, geomorphological and biological applications. *Hydrological Processes* 5: 3–30.

Morozov VP (1979) *A Course in Spheroidal Geodesy*, 2nd edn. Moscow: Nedra (in Russian).

Mynatt I, Bergbauer S and Pollard DD (2007) Using differential geometry to describe 3D folds. *Journal of Structural Geology* 29: 1256–1266.

Olson CJ, Becker JJ and Sandwell DT (2014) A new global bathymetry map at 15 arcsecond resolution for resolving seafloor fabric: SRTM15_PLUS. In: *American Geophysical Union, Fall Meeting 2014*, San Francisco, CA, 15–19 December 2014. Washington, DC: American Geophysical Union: # OS34A–03.

Omelko AM, Krestov PV and Yakovleva AN (2012) A topography-based model of the vegetation cover of the Lanzhinskie mountains. *Botanica Pacifica* 1: 109–119.

Orlandini S, Moretti G, Corticelli MA, et al. (2012) Evaluation of flow direction methods against field observations of overland flow dispersion. *Water Resources Research* 48: W10523.

Orlandini S, Moretti G and Gavioli A (2014) Analytical basis for determining slope lines in grid digital elevation models. *Water Resources Research* 50: 526–539.

Pacina J (2010) Comparison of approximation methods for partial derivatives of surfaces on regular grids. *Geomorphologia Slovaca et Bohemica* 1(10): 25–32.

Panou G (2013) The geodesic boundary value problem and its solution on a triaxial ellipsoid. *Journal of Geodetic Science* 3: 240–249.

Peckham SD (2013) Mathematical surfaces for which specific and total contributing area can be computed: Testing contributing area algorithms. In: *Proceedings of Geomorphometry 2013*, Nanjing, China, 16–20 October 2013. Geomorphometry.org: # O–11.

Pike RJ (2000) Geomorphometry: Diversity in quantitative surface analysis. *Progress in Physical Geography* 24: 1–20.

Pogorelov AV (1957) *Differential Geometry*. Groningen, the Netherlands: Noordhoff.

Prasicek G, Otto JC, Montgomery DR, et al. (2014) Multi-scale curvature for automated identification of glaciated mountain landscapes. *Geomorphology* 209: 53–65.

Quinn PF, Beven KJ, Chevallier P, et al. (1991) The prediction of hillslope flowpaths for distributed modelling using digital terrain models. *Hydrological Processes* 5: 59–80.

Roberts A (2001) Curvature attributes and their application to 3D interpreted horizons. *First Break* 19: 85–100.

Rosenberg P (1955) Information theory and electronic photogrammetry. *Photogrammetric Engineering* 21: 543–555.

Rothe R (1915) Zum problem des talwegs. *Sitzungsberichte der Berliner Mathematischen Gesellschaft* 14: 51–68.

Schmidt J, Evans IS and Brinkmann J (2003) Comparison of polynomial models for land surface curvature calculation. *International Journal of Geographical Information Science* 17: 797–814.

Sharaya LS and Shary PA (2011) Geomorphometric study of the spatial organization of forest ecosystems. *Russian Journal of Ecology* 42: 1–8.

Shary PA (1991) The second derivative topographic method. In: Stepanov IN (ed) *The Geometry of the Earth Surface Structures*. Pushchino, USSR: Pushchino Research Centre Press, 30–60 (in Russian).

Shary PA (1995) Land surface in gravity points classification by a complete system of curvatures. *Mathematical Geology* 27: 373–390.

Shary PA (2008) Models of topography. In: Zhou Q, Lees B and Tang G-A (eds) *Advances in Digital Terrain Analysis*. Berlin: Springer, 29–57.

Shary PA and Pinskii DL (2013) Statistical evaluation of the relationships between spatial variability in the organic carbon content in gray forest soils, soil density, concentrations of heavy metals and topography. *Eurasian Soil Science* 46: 1076–1087.

Shary PA and Smirnov NS (2013) Mechanisms of the effects of solar radiation and terrain anisotropy on the vegetation of dark conifer forests in the Pechora–Ilych State Biosphere Reserve. *Russian Journal of Ecology* 44: 9–17.

Shary PA and Stepanov IN (1991) Application of the method of second derivatives in geology. *Transactions (Doklady) of the USSR Academy of Sciences, Earth Science Sections* 320: 87–92.

Shary PA, Rukhovich OV and Sharaya LS (2016) Analytical and cartographic predictive modeling of arable land productivity. In: Mueller L, Sheudshen AK and Eulenstein F (eds) *Novel Methods for Monitoring and Managing Land and Water Resources in Siberia*. Cham, Switzerland: Springer, 489–502.

Shary PA, Sharaya LS and Mitusov AV (2002) Fundamental quantitative methods of land surface analysis. *Geoderma* 107: 1–32.

Shary PA, Sharaya LS and Mitusov AV (2005) The problem of scale-specific and scale-free approaches in geomorphometry. *Geografia Fisica e Dinamica Quaternaria* 28: 81–101.

Shebuev GN (1896) Geometric bases of geodesy on a triaxial ellipsoid, very little different from a spheroid. *Proceedings of the Topographic-Geodetic Commission* 5: 70–97 (in Russian).

Sjöberg LE (2006) New solutions to the direct and indirect geodetic problems on the ellipsoid. *Zeitschrift für Vermessungswesen* 131: 35–39.

Smith DE, Zuber MT, Neumann GA, et al. (2010) Initial observations from the Lunar Orbiter Laser Altimeter. *Geophysical Research Letters* 37: L18204.

Smith DE, Zuber MT, Solomon SC, et al. (1999) The global topography of Mars and implications for surface evolution. *Science* 284: 1495–1503.

Smith MW, Carrivick JL and Quincey DJ (2016) Structure from motion photogrammetry in physical geography. *Progress in Physical Geography* 40: 247–275.

Speight JG (1974) A parametric approach to landform regions. In: Brown EH and Waters RS (eds) *Progress in Geomorphology: Papers in honour of DL Linton*. London: Institute of British Geographers, 213–230.

Stewart SA and Podolski R (1998) Curvature analysis of gridded geological surfaces. *Geological Society of London Special Publications* 127: 133–147.

Stooke PJ (1998) Mapping worlds with irregular shapes. *Canadian Geographer* 42: 61–78.

Strahler AN (1957) Quantitative analysis of watershed geomorphology. *Transactions of the American Geophysical Union* 38: 913–920.

Stumpf F, Schmidt K, Goebes P, et al. (2017) Uncertainty-guided sampling to improve digital soil maps. *Catena* 153: 30–38.

Tadono T, Ishida H, Oda F, et al. (2014) Precise global DEM generation by ALOS PRISM. *ISPRS Annals of the Photogrammetry, Remote Sensing and Spatial Information Sciences* II(4): 71–76.

Tarboton DG (1997) A new method for the determination of flow directions and upslope areas in grid digital elevation models. *Water Resources Research* 33: 309–319.

Tarolli P (2014) High-resolution topography for understanding Earth surface processes: Opportunities and challenges. *Geomorphology* 216: 295–312.

Temovski M and Milevski I (2015) DEM based geomorphometric analyses of karst surface in the Republic of Macedonia. In: Jasiewicz J, Zwoliński Z, Mitášová H, et al. (eds) *Geomorphometry for Geosciences*. Poznań, Poland: Institute of Geoecology and Geoinformation, 65–68.

Thomas PC (1989) The shapes of small satellites. *Icarus* 77: 248–274.

Toutin T (2008) ASTER DEMs for geomatic and geoscientific applications: A review. *International Journal of Remote Sensing* 29: 1855–1875.

Trevisani S and Rocca M (2015) MAD: Robust image texture analysis for applications in high resolution geomorphometry. *Computers and Geosciences* 81: 78–92.

Tribe A (1992) Automated recognition of valley lines and drainage networks from grid digital elevation models: A review and a new method. *Journal of Hydrology* 139: 263–293.

USGS (2015) *Earth Explorer*. Sioux Fall, SD: EROS Center, US Geological Survey. Available at: http://earthexplorer.usgs.gov (accessed 13 September 2017).

Vincenty T (1975) Direct and inverse solutions of geodesics on the ellipsoid with application of nested equations. *Survey Review* 23: 88–93.

Volkov NM (1950) *Principles and Methods of Cartometry*. Moscow: Soviet Academic Press (in Russian).

Wasklewicz T, Staley DM, Reavis K, et al. (2013) Digital terrain modeling. In: Bishop MP (ed) *Treatise on Geomorphology*. Vol. 3: *Remote sensing and GIScience in geomorphology*. London: Academic Press, 130–161.

Weatherall P, Jakobsson M and Marks KM (2014) General Bathymetric Chart of the Oceans (GEBCO): Mapping the global seafloor. In: *Fall Meeting 2014, American Geophysical Union*, San Francisco, CA, 15–19 December 2014. Washington, DC: American Geophysical Union: # OS31B–0990.

Wilson JP (2012) Digital terrain modeling. *Geomorphology* 137: 107–121.

Wilson JP and Gallant JC (eds) (2000) *Terrain Analysis: Principles and applications*. New York: J Wiley & Son.

Wilson JP, Aggett G, Deng Y, et al. (2008) Water in the landscape: A review of contemporary flow routing algorithms. In: Zhou Q, Lees B and Tang G-A (eds) *Advances in Digital Terrain Analysis*. Berlin: Springer, 213–236.

Xu T, Moore ID and Gallant JC (1993) Fractals, fractal dimensions and landscapes: A review. *Geomorphology* 8: 245–262.

Yokoyama R, Shirasawa M and Pike RJ (2002) Visualizing topography by openness: A new application of image processing to digital elevation models. *Photogrammetric Engineering and Remote Sensing* 68: 257–265.

Young T (1805) An essay on the cohesion of fluids. *Philosophical Transactions of the Royal Society of London Pt I* 95: 65–87.

Zevenbergen LW and Thorne CR (1987) Quantitative analysis of land surface topography. *Earth Surface Processes and Landforms* 12: 47–56.

Zink M, Bachmann M, Brautigam B, et al. (2014) TanDEM-X: The new global DEM takes shape. *IEEE Geoscience and Remote Sensing Magazine* 2: 8–23.